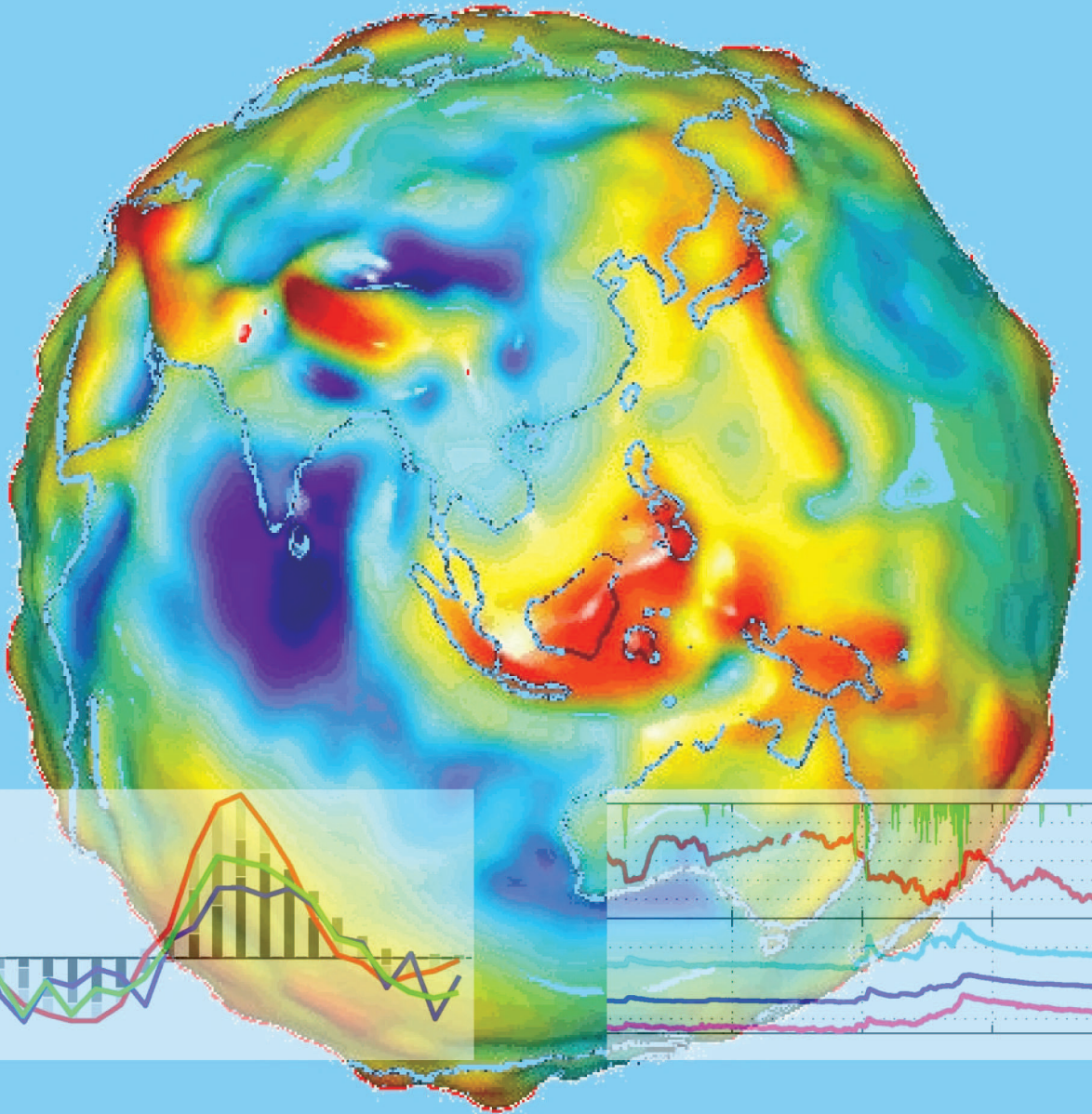


Terrestrial water storage change from temporal gravity variation



Shaakeel Hasan

Terrestrial water storage change from temporal gravity variation

Shaakeel Hasan

Promotoren:

Prof. dr. ir. P.A. Troch
Hoogleraar Hydrologie en Kwantitatief Waterbeheer (1999–2005),
Wageningen Universiteit
en
Professor of Hydrology and Water Resources
Professor of Civil Engineering and Engineering Mechanics
University of Arizona (Tucson, AZ, USA)

Prof. dr. ir. R. Uijlenhoet
Hoogleraar Hydrologie en Kwantitatief Waterbeheer
Wageningen Universiteit

Promotiecommissie:

Prof. Dr.-Ing. habil. R. Klees, Technische Universiteit Delft
Prof. dr. ir. H.H.G. Savenije, Technische Universiteit Delft
Prof. dr. ir. M.F.P. Bierkens, Universiteit Utrecht
Prof. dr. ir. S.E.A.T.M. van der Zee, Wageningen Universiteit

Dit onderzoek is uitgevoerd binnen de onderzoekschool SENSE

Terrestrial water storage change from temporal gravity variation

Shaakeel Hasan

Proefschrift
ter verkrijging van de graad van doctor
op gezag van de rector magnificus
van Wageningen Universiteit,
Prof. dr. M.J. Kropff,
in het openbaar te verdedigen
op maandag 27 april 2009
des namiddags te vier uur in de Aula.

Shaakeel Hasan, 2009

Terrestrial water storage change from temporal gravity variation

Ph.D. thesis, Wageningen University, Netherlands
With summaries in English and Dutch

ISBN 978-90-8585-385-5

Abstract

Recent progress in accurately monitoring temporal gravity variations by means of superconducting gravimeters and satellite geodesy provides unprecedented opportunities in closing the water balance. This thesis deals with the relation between temporal gravity variation and water storage change.

A superconducting gravimeter observes with high accuracy (few nm/s^2) and high frequency (1 Hz) the temporal variations in the Earth's gravity field, in Moxa, Germany. Hourly gravity residuals are obtained by time-averaging and correcting for Earth tides, polar motion, barometric pressure variations, and instrumental drift. These gravity residuals are significantly affected by hydrological processes (interception, infiltration, surface runoff and subsurface redistribution) in the vicinity of the gravimeter. First, time series analysis and distributed hydrological modeling techniques were applied to investigate the effect of hydrological processes on observed terrestrial gravity residuals. It is shown that the short-term response of gravity residuals to medium to heavy rainfall events can be efficiently modeled by means of a linear transfer function. This transfer function exhibits an oscillatory behavior that indicates fast redistribution of stored water in the upper layers (interception store, root zone) of the catchment surrounding the instrument. The relation between groundwater storage and gravity residuals is less clear and varies according to the season. High positive correlation between groundwater and gravity exists during the winter months when the freezing of the upper soil layers immobilizes water stored in the unsaturated zone of the catchment. Similar results are found in the application of a distributed hydrological model to detect gravity variation. Observed gravity change is then considered as an integrator of catchment-scale hydrological response (similar in nature to discharge measurements), and therefore used to constrain catchment-scale hydrologic models. Results indicate that a lumped water balance model for unsaturated storage and fluxes, coupled with a semi-distributed hydraulic groundwater model for saturated storage and fluxes, successfully reproduces both gravity and discharge dynamics.

Since its launch, the Gravity Recovery and Climate Experiment (GRACE) mission has been providing estimates of surface mass anomalies for the entire globe. Despite the coarse spatial (a few hundred kilometers) and temporal (1 month) resolution, the mission has proven to deliver valuable data for continental scale river basin water balance studies. Recently released GRACE gravity field coefficients represent a significant improvement over previous releases. The potential of such distributed GRACE measurements is investigated in a smaller, partly mountainous, partly semi-arid basin, namely the Colorado River Basin (CRB). For the period 2003-2005, monthly 1 degree GRACE data from different releases are correlated with different spatial distributions of hydrologic simulations (VIC model) and in-situ observations. High spatial correlations between VIC and GRACE are found for most of the CRB, where snow and groundwater dominate the Upper and Lower CRB respectively, and soil moisture affects the entire CRB. Results show the need to combine hydrological information from the surrounding basins to apply GRACE data in a basin like CRB. The differences in various GRACE products for the same basin also need to be addressed.

Preface

I do not remember when for the first time I learned or understood the concept of gravity. However, I do remember some of my childhood (boyhood) fantasies, specially the one regarding getting rid of the force binding me – I wanted to fly away, escaping gravity. It took some time to accept that gravity practically binds me to the earth, but I never thought gravity would bind me theoretically as well. As Tagore sings, “I can, in my heart, go anywhere I like”, I wanted to live like that. In practice, instead of going anywhere, I went for becoming a civil engineer. Once I got there, I decided for water resource engineering. It did not stop, as I wanted to master the computational or modeling part of water. So, after some years of working I got back to school that brought me to the world of research. My interest grew towards hydrology, and when I got a job in Wageningen University to do a Ph.D. research, there came the link to gravity. And despite of my wish to escape any binding force, it was simply wonderful to connect my field (hydrology) with gravity.

Peter, it is indeed a great privilege to get you as my promoter and to do this job under your supervision. I appreciate your professional quality as well as your personality. You did not bind me, instead you gave me freedom, encouraging me to explore in my own ways. Working (discussing) with you always brought me new ideas. Just talking to you was simply fun. I could even understand your Dutch (Flemish) better than other Dutch. There were times, I had difficulties in my work, but talking to you was always a great solution. I remember calling it your magic. I do not think I can thank you enough for all what you did for me.

Remko, during most of my contract, you were more a neighbor (at office) than my promoter. We had some unofficial talks at times, however, that did not concern much of my research developments. After you became the professor of the Hydrology and Quantitative Water Management group, you rightly took responsibilities and I got your ears bringing me extra support in my research. It was for a short period, but you played a big role in my progress. I am

extremely grateful to you.

During all these years, I came across many people at different places, and they made important contributions to my research. I would like to thank all of them. I thank Jan Boll (for SMR model, field trips and the squash lesson), Eric Wood (field trip), Jay Famiglietti (for hosting me at UCI), and Corinna Kroner (for the fruitful collaboration that extends to my group).

Twice, I spent 4 to 6 weeks in Tucson. I kindly acknowledge Horton Research Grant from AGU for its encouragement and making extra trips possible. Both the trips were great, not only because I had a chance to get Peter, but also because I came across nice people. I really felt at home with Monica and Peter. Thanks Peter and Monica, I still hope to host the two of you some time, somewhere. Also thanks to Alex, Pieter, Maite, Mare, Latfi and Matej.

I enjoyed having great colleagues. I did not have much scope for joint research with my colleagues, but the breaks and trips were great. Coffee breaks with Ryan, Hidde, Remko, Remco, Alexis, Tessa and Ruud and fresh air breaks with Arno and Tessa were wonderful. Patrick and Hidde gave smart programming solutions, Paul gave books, Roel and Henny accompanied me to Moxa, Magda digged books for our need, Henny and Annemarie took care of everything else. I appreciate the interest of my colleagues in my work and in me personally.

I acknowledge my relatives and friends, who offered good care, listening ears and supports. They even agreed not to ask me about the date, when I got too delayed. I am grateful to Catharien's family. The short, but regular, family visits to or from Friesland, were great for breaks. Heit en Mem, thank you for providing me extra time and conditions to work, by taking care of my family.

I do not have words to acknowledge the contribution of my family (Abbu, Mamoni, Dada, Bubu, Mejda, Seena). From a very early stage in life, you always gave me space for what and how I think about things. Without you, I would not be where I am today. I love you.

Catharien, other than Remko and Peter, you are the first person to read each and every word of my thesis. You along with the children had to sacrifice a lot for my work and development. We have gone through days with worries and challenges of different scales, but at the end we always manage to smile. You are a champion.

Akash and Minke, you had to wait a long time for me to finish this book. You both did a good job by accepting me being busy with work and bringing me smiles, happiness and strength. Yet, you are capable of making me forgetting everything else. I am so very proud of you.

Shaakeel Hasan
Wageningen, April 2009

Contents

1	Introduction	1
1.1	Background	1
1.2	Terrestrial gravity	2
1.2.1	Temporal variation of terrestrial gravity	3
1.2.2	Superconducting gravimeter	4
1.3	Satellite geodesy	5
1.3.1	GRACE twin satellites	5
1.3.2	GRACE gravity field	6
1.3.3	Limitations	7
1.4	Problem description	7
1.5	Thesis outline	8
2	Time series analysis and modeling of terrestrial gravity	11
2.1	Introduction	11
2.2	Data and methods	12
2.3	Precipitation and gravity	12
2.4	Groundwater and gravity	16
2.5	Discussion	18
3	Distributed hydrology to model terrestrial gravity variation	19
3.1	Introduction	19
3.2	Study area	20
3.2.1	Location and background	20
3.2.2	Geophysical characteristics	22
3.2.3	Hydrometeorological characteristics	22
3.3	Data	22

3.3.1	Gravity	22
3.3.2	Hydrometeorology	22
3.3.3	Auxiliary data	27
3.4	Soil Moisture Routing (SMR) model	27
3.5	Analysis and results	28
3.6	Discussion	31
4	Application of terrestrial gravity variation in hydrological modeling	33
4.1	Introduction	33
4.2	Modeling approach	34
4.2.1	Gravity model	35
4.2.2	Hydrological model	36
4.2.3	Model input and conditions	39
4.3	Sensitivity analysis of local gravity variation	41
4.4	Gravity variation and hydrology	43
4.4.1	Fast storage change	43
4.4.2	Slow storage change	47
4.4.3	Hydrological gravity reductions	48
4.4.4	Final model output	48
4.5	Discussion	48
5	Potential of satellite gravity measurements in hydrological modeling	51
5.1	Introduction	51
5.2	Materials and methods	52
5.2.1	The Gravity Recovery and Climate Experiment	52
5.2.2	Hydrological modeling	54
5.2.3	In-situ data sets	55
5.3	Analysis and results	55
5.3.1	Basin average GRACE and VIC	55
5.3.2	Distributed GRACE	58
5.3.3	Distributed GRACE and observed data	62
5.3.4	Potential of GRACE data	62
5.4	Discussion	64
6	Synthesis	65
6.1	Conclusions	65
6.1.1	Terrestrial gravity	65
6.1.2	Satellite geodesy	66
6.2	General discussion	67
6.2.1	Terrestrial gravity	67
6.2.2	Satellite geodesy	69
6.3	Perspectives	69

Bibliography	71
Summary	77
Samenvatting	79
PhD training program	81
Curriculum Vitae	83

List of Tables

4.1 Parameters of the water balance model	39
4.2 Parameters for lumped water balance model	45
4.3 Parameters for semi-distributed hsB model	47
5.1 Correlation between VIC and GRACE	56
5.2 Correlation between VIC, GRACE and in-situ data	62

List of Figures

1.1	Non-tidal gravity variations	4
1.2	A superconducting gravimeter	5
2.1	Exploration of gravity residuals	13
2.2	Impulse response function	15
2.3	Exploration of groundwater and gravity	17
3.1	Silberleite catchment	21
3.2	Gravity reductions	23
3.3	Exploration of precipitation	24
3.4	From illuminance to solar radiation	25
3.5	Stage-discharge relationship	26
3.6	Soil Moisture Routing model	27
3.7	Modeling gravity variation	30
3.8	Exploration of domains and storage componets	31
4.1	Gravity model (sketch)	35
4.2	Hydrological processes (scheme)	36
4.3	From catchment to hillslopes	40
4.4	Effects of fast storage change	41
4.5	Analysis of slow storage change	42
4.6	Modeling fast gravity variation	44
4.7	Effects of saturated water storage change	45
4.8	Range of gravity variation for varying bedrock depth	46
4.9	Observed and modeled discharge	49
5.1	Colorado River basin	53
5.2	Variable Infiltration Capacity (VIC) model (scheme)	54
5.3	Basin average surface mass anomaly from GRACE	56
5.4	Comparison between GRACE and VIC	57
5.5	Maps of mean surface mass anomaly from distributed GRACE	59
5.6	Maps of variation in surface mass anomaly from distributed GRACE	60
5.7	Comparison between GRACE and VIC for the Upper and Lower Colorado	61
5.8	Comparison between GRACE and observed snow	61
5.9	Correlation between GRACE and VIC	63

CHAPTER 1

Introduction

1.1 Background

Hydrology plays an important role in the dynamic system of the earth. This system consists of a fluid and mobile atmosphere and oceans, and a continuously changing distribution of ice, snow, soil moisture and groundwater, which are components of the water cycle. All these changes affect the distribution of mass in the earth and produce variations in the earth's gravitational field on a variety of spatial and temporal scales. Highly accurate measurements of the earth's gravity field made with appropriate spatial and temporal sampling can thus be used to better understand the processes that move mass within the earth, and on and above its surface.

Traditionally, the gravity field has been treated as essentially steady-state because 99% of the departure of the field from a rotating fluid figure of the earth's mass is static in historic time. The static field is dominated by irregularities in the solid earth caused by convective processes that deform the solid earth on time scales of thousands to millions of years. The next generation of gravimeters (both in-situ and satellite based) is however envisioned to meet the need of the remaining 1% of the departure of the gravity field, which is caused by processes that vary on time scales ranging from hours to thousands of years (*NRC*, 1997).

Temporal variations are caused by a variety of phenomena that redistribute mass, including tides raised by the sun and the moon, and post-glacial rebound (i.e., creep in the mantle in response to the geologically recent removal of ice sheets). The hydrosphere - oceans, lakes, groundwater, soil moisture - is the other source of much of the irregular variations in the time-varying mass distribution from sub-daily to long-term (aquifer depletion) periods. Particu-

larly exciting is the potential to study changes in terrestrial water storage by investigating temporal gravity variations.

Hydrological study is currently going through a revolution, in which a multitude of new data and knowledge from other branches of geoscience are being applied, explored, and tested (e.g. *Krajewski et al. (2006)*; *Alsdorf and Lettenmaier (2003)*). One example of these new kinds of data is highly accurate temporal gravity variation from both terrestrial and satellite observations.

Gravity, the oldest force known to mankind, is in many ways also the youngest. It is understood well enough to explain stars, black holes and the Big Bang, and yet in some ways it is not understood at all (*Schutz, 2003*). Gravity, the universal force of attraction that affects all matter, is the weakest of the four basic physical forces (the others being the electromagnetic force, and the strong and weak nuclear binding forces), but this is the one that influences nearly all physical, chemical, and biological processes on earth. The knowledge of gravity and its spatio-temporal variability, in particular its spatial variation, is being used in many branches of science and the earth's exploration. Recent progress in accurately monitoring temporal gravity variations by means of superconducting gravimeters and satellite geodesy has brought a complete new avenue of estimating water storage changes (e.g. *Wahr et al. (2004)*; *Hasan et al. (2008)*).

Application of gravity observations in hydrological studies is still in its infancy. However, studies related to finding the hydrological effect on gravity variation promise significant potential in observing hydrologic state variables and fluxes at different scales. In the following sections, we will introduce the basics of terrestrial gravity and satellite geodesy for hydrology.

1.2 Terrestrial gravity

The force exerted on an element of mass at the surface of the earth has two principal components: (1) gravitational attraction of the mass of the earth, and (2) rotation of the earth. Gravity refers to the combined effects of both gravitation and rotation. If the earth were a non-rotating spherically symmetric body, the gravitational acceleration on its surface would be constant. However, because of the earth's rotation, topography and internal lateral density variations, the acceleration of gravity g varies with location on the surface. The earth's rotation leads mainly to a latitude dependence of the surface gravitational acceleration. As rotation distorts the surface by producing an equatorial bulge and a polar flattening, gravity at the equator is about 0.5% less than gravity at the poles. Topography and density inhomogeneities in the earth lead to spatial variations in surface gravity (*Turcotte and Schubert, 2002*). While geophysical properties are responsible for spatial variation of gravity, the temporal gravity variation is caused by geodynamic processes.

1.2.1 Temporal variation of terrestrial gravity

Temporal gravity variations may be divided into effects due to a time dependent gravitational constant and variations of the earth's rotation, tidal accelerations, and variations caused by terrestrial mass displacements (redistribution). The latter is interesting for hydrology, as water plays an important role in terrestrial mass redistribution. However, to infer the temporal variation of gravity components, caused by hydrological dynamics, all the other known effects have to be subtracted from measured gravity variation. In the following paragraphs, we will briefly discuss the main factors causing temporal gravity variation.

Earth and ocean tide: On the one hand the gravitational attraction of celestial bodies (moon, sun, planets) causes earth and ocean tides of different periods and amplitudes. On the other hand, mass displacement and deformation of the earth's surface caused by tidal forces cause changes in gravity. Basically, the tidal forces have the strongest effect on gravity (see Figure 3.2). In geodesy, computations are carried out separately for the individual two-body systems (earth-moon, earth-sun, etc.) and the results are subsequently added, with the celestial bodies regarded as point masses (*Torge, 2001*).

Atmospheric pressure: Atmospheric pressure variations affect gravimeter output in two ways: directly by gravitational attraction of the atmospheric mass and indirectly by the deformation effect. There are various ways to correct for atmospheric pressure effects. *Kroner and Jentzsch (1999)* give a comparison of different barometric pressure reductions for gravity data and resulting consequences.

Polar motion: The direction of the earth's axis of rotation is not rigorously fixed, neither in space nor with respect to the earth, but undergoes very small, more or less periodic variations. Astronomers know it by the name of nutation (with respect to inertial space), geodesists know it by the name of polar motion (with respect to the earth's body). This phenomenon arises from a minute difference between the axes of rotation and of maximum inertia, the angle between these axes being about $0.3''$. This motion of the pole has a main period of about 430 days, the Chandler period, but is rather irregular, presumably because of the movement of masses, atmospheric variations, etc.

Instrumental effects: Depending on the type of gravimeter, there can be different instrumental effects on gravity measurements. For example, the accuracy of spring gravimeters will deteriorate with time, by the deterioration of elasticity. Superconducting gravimeters are known to give long-term stability. However, regular calibration and comparison with absolute gravimeter measurements are needed to ensure data quality.

Temporal gravity changes caused by terrestrial mass displacements can occur in various forms: abrupt, periodic or quasi-periodic, and secular. Their

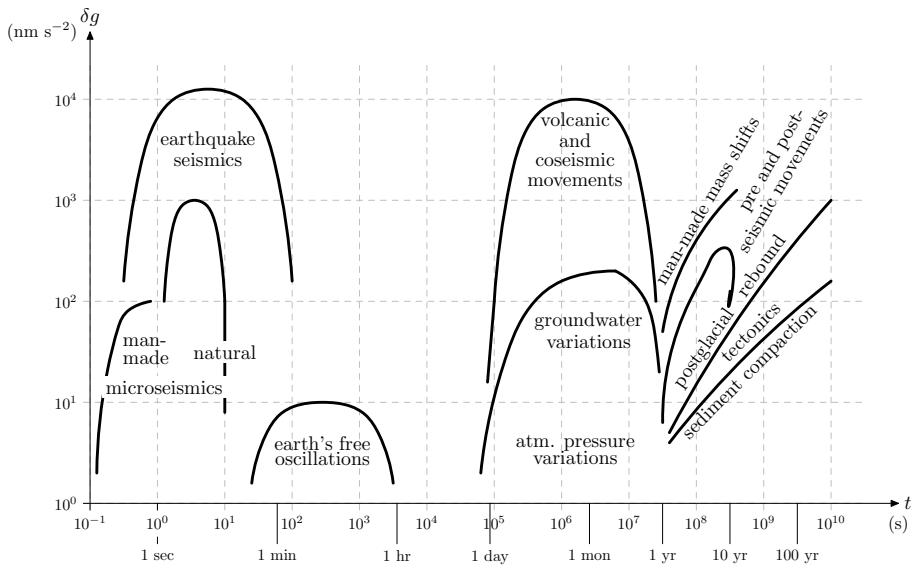


Figure 1.1: Non-tidal gravity variations produced by terrestrial mass displacements (*Torge, 1989*).

effect at the earth's surface can be local, regional, or global, whereby the depth of the source of the gravity change generally increases with the size of the affected area. In general, long-term forces cause viscous deformations, whereas short-term (quasi-) periodic forces cause elastic deformations. Abrupt local processes mostly lead to permanent changes. Figure 1.1 gives an overview of the extent and course of some of the above mentioned processes.

1.2.2 Superconducting gravimeter

Changes in gravity with time can be detected by repeated gravity measurements. A high measurement accuracy is required for this purpose, and the repetition rate has to be adapted to the temporal evolution (its period, as shown in Figure 1.1) of the gravity change. Superconducting gravimeters (SG), providing nm s^{-2} accuracy in short-term (e.g. hourly) gravity changes and long-term stability, are suitable devices to monitor temporal gravity variation with high accuracy (*Goodkind, 1999*). A superconducting gravimeter (Figure 1.2) consists of a hollow superconducting sphere that levitates in a persistent magnetic field. The almost frictionless bearing of the mass and the stability of the magnetic field generated by superconducting coils provide a highly sensitive gravimeter which is stable for long periods. An electrostatic capacitive device detects the vertical position changes of the levitating sphere and a magnetic feedback force maintains the sphere at a fixed position. SGs are equipped with an electronics card (gravity control card) that contains the feedback integrator whose voltage is proportional to acceleration changes.



Figure 1.2: The superconducting gravimeter at the Geodynamic Observatory Moxa, Germany.

1.3 Satellite geodesy

In a nutshell, geodesy is the study of the measurement and mapping of the earth's surface. One of the basic problems in geodesy is determination of the earth's gravity field and linear functions of this field (e.g. a precise geoid, which is the equipotential surface of the earth's gravity field). Satellite geodesy comprises the observational and computational techniques, which allow the solution of geodetic problems by the use of precise measurements to, from, or between artificial, mostly near-earth, satellites. The main idea is to detect the deviation, caused by the earth's gravity, of an orbiting satellite from its designed orbit at a certain instant of time to infer to the geoid anomaly (from the time or space averaged geoid) at that time. The twin satellites from the Gravity Recovery and Climate Experiment (GRACE) are an example of such a system to measure the geoid anomaly.

1.3.1 GRACE twin satellites

The primary objective of the GRACE mission is to obtain accurate estimates of the mean and time-variable components of the earth's gravity field variations. This objective is achieved by making continuous measurements of the change in distance between a twin spacecraft, co-orbiting at ~ 500 km altitude, in a near circular, polar orbit, spaced ~ 220 km apart, using a microwave ranging system. In addition to this range change, the non-gravitational forces are measured on each satellite using a high-accuracy electrostatic, room-temperature accelerometer. The satellite orientation and position (and timing) are precisely measured using twin star cameras and a GPS receiver, respectively. Spatial and temporal variations in the earth's gravity field affect the orbits (or trajectories)

of the twin spacecraft differently. These differences are manifested as changes in the distance between the spacecraft, as they orbit the earth. This change in distance is reflected in the time-of-flight of microwave signals transmitted and received nearly simultaneously between the two spacecraft. The change in this time of flight is continuously measured by tracking the phase of the microwave carrier signals. The so-called dual-one-way range change measurements can be reconstructed from these phase measurements. This range change (or its numerically inferred derivatives), along with other mission and ancillary data, is subsequently analyzed to extract the parameters of an earth gravity field model.

1.3.2 GRACE gravity field

Usually the earth's global gravity field is represented in terms of the shape of the geoid, the equipotential surface that most closely coincides with the mean sea level over the ocean. The geoid N can be expanded as a sum of spherical harmonics:

$$N(\theta, \phi) = a \sum_{l=0}^{\infty} \sum_{m=0}^l \tilde{P}_{lm}(\cos \theta) \{C_{lm} \cos(m\phi) + S_{lm} \sin(m\phi)\} \quad (1.1)$$

where θ is colatitude, ϕ is longitude, a is the mean radius of the earth, and C_{lm} and S_{lm} are dimensionless Stokes coefficients for degree l and order m of the harmonic function. The degree l is a measure of the spatial scale of a spherical harmonic. The half wavelength of a spherical harmonic (of degree l and order m) serves as an approximate representation of the spatial scale and is roughly $20,000/l$ km. The higher the degree l , the finer the spatial resolution. The order m describes the amplitude of the harmonic component. The \tilde{P}_{lm} are normalized associated Legendre functions:

$$\tilde{P}_{lm}(x) = \sqrt{(2 - \delta_{m0})(2l + 1)} \frac{(l - m)!}{(l + m)!} \times \frac{(1 - x^2)^{\frac{m}{2}}}{2^l l!} \frac{d^{l+m}}{dx^{l+m}} (x^2 - 1)^l \quad (1.2)$$

Supposing ΔN as change in the geoid, ΔN can be represented in terms of changes, ΔC_{lm} and ΔS_{lm} , in the spherical harmonic geoid coefficients:

$$\Delta N(\theta, \phi) = a \sum_{l=0}^{\infty} \sum_{m=0}^l \tilde{P}_{lm}(\cos \theta) \{\Delta C_{lm} \cos(m\phi) + \Delta S_{lm} \sin(m\phi)\} \quad (1.3)$$

The ΔN is related to change in density redistribution in a thin layer of the earth's surface, causing the change in geoid. As the surface mass also loads and deforms the underlying solid earth, there will be an additional geoid change, which can be taken care of applying k_l , the load Love number of degree l (see e.g. *Farrell (1972)* and *Chao (1994)*). The final equation expressing the

relation between change in surface density, $\Delta\sigma$ (mainly caused by redistribution of liquid water) and the changes of the Stokes coefficients ΔC_{lm} and ΔS_{lm} is:

$$\Delta\sigma(\theta, \phi) = \frac{a\rho_{ave}}{3} \sum_{l=0}^{\infty} \sum_{m=0}^l \tilde{P}_{lm}(\cos\theta) \frac{2l+1}{1+k_l} \{\Delta C_{lm} \cos(m\phi) + \Delta S_{lm} \sin(m\phi)\} \quad (1.4)$$

where ρ_{ave} is the average density of the earth (5517 kg/m³). We refer the reader to *Wahr et al. (1998)* for more details on time-variable gravity recovery from GRACE.

1.3.3 Limitations

In applying load Love numbers k_l to consider changes in geoid caused by deformation due to load, there can be errors if k_l is not calculated exactly. Calculated values of k_l for some degree l are available in different publications (*Wahr et al., 1998*), and in general the values in between are linearly interpolated. Linearly interpolating the available values instead of using exact results introduces errors of less than 0.05% for all $l < 200$.

The above mentioned results assume a surface mass layer thin enough to ensure that $(l+2)H/a \ll 1$ for $l \leq l_{max}$, where H is the thickness of the layer. For the atmosphere, most of the mass lies within 10 km of sea level. As an example, for $H = 10$ km and $l = 60$, $(l+2)H/a \approx 0.1$. This ratio is not small enough for the thin layer assumption to be adequate for atmospheric applications.

The $l = 0$ term is proportional to the total mass (solid earth and its fluid envelope) of the earth. This total mass does not change with time, and so ΔC_{00} from GRACE can be assumed to vanish. However, if the geoid contribution of one component (e.g. the ocean) of surface mass is considered, this mass can be variable. So the oceanic contributions to ΔC_{00} need not vanish.

The $l = 1$ terms are proportional to the position of the earth's center of mass relative to the center of the coordinate system and so depend on how the coordinate system is chosen. If the coordinate system is chosen such that the origin always coincides with the earth's instantaneous center of mass, all $l = 1$ terms in the geoid are zero by definition. Hence for GRACE $\Delta C_{lm} = \Delta S_{lm} = 0$ for all $l = 1$. Again the $l = 1$ coefficients for an individual component of the total surface mass need not vanish.

1.4 Problem description

Terrestrial water storage is a key factor in the hydrological balance and of direct influence to processes like evapotranspiration and percolation. Therefore it plays a major role in climate modeling and water management issues. Routine observation of soil moisture or groundwater is still done at the point scale. There is an urgent need for detection methods on a larger scale. Some progress

has been made regarding the application of remote sensing techniques, such as passive and active microwave observations of the earth's surface (*Verhoest et al.*, 1998; *Mancini et al.*, 1999). Although these methods provide spatial information about soil moisture, they do so only at the upper surface of the soil profile. Gravity information can open a new route towards solving this important issue for hydrological and climate modeling.

The Global Geodynamics Project (GGP) (*Crossley et al.*, 1999) began in 1997 with one of the purposes being to record the earth's gravity field with extremely high accuracy (temporal variation with an accuracy of $\sim 10^{-9} \text{ m s}^{-2}$) at a number of stations around the world using superconducting gravimeters (SGs). The SG network of the GGP provides hydrologists with the appropriate baseline data to study the local and regional impact of hydrological phenomena on the gravity field. Since its launch in March 2002, the Gravity Recovery and Climate Experiment (GRACE) (*Tapley et al.*, 2004b) mission has been providing estimates of surface mass anomalies for the entire globe. The GRACE data and its sub-products are publicly available through Internet, providing data for basin scale hydrological studies. Both GGP and GRACE recognize that tracking the movement of water on and beneath the earth surface is one of the main goals and thus promise a significant contribution to hydrological studies.

Any gravity measurement, be it terrestrial or space-based, cannot, by itself, discriminate between changes in water on the surface, in the soil, or in the groundwater table. Instead, such measurements provide constraints on changes of the total water in vertical columns, integrated from the earth's surface down through the base of the water table. Furthermore, the partitioning of water storage changes among different storage components is not sufficiently known. Nevertheless, the direct measurement of water storage changes by gravity field measurements is of great potential in the field of hydrology in order to close the water balance at different scales in space and time, and to validate and improve the predictive capacity of hydrological models.

Although the relationship between time-variable gravity and water storage is well established, application of gravity observations in hydrological modeling is still in its infancy. This thesis aims at investigating the possibility to detect variations in terrestrial water storage from measurements of the time dependent gravity field, and to assess the accuracy of these estimations based on terrestrial and satellite observations of the gravity field. The hypothesis is that temporally variable gravity measurements, both terrestrial and satellite based, contain valuable information about water storage in surface and subsurface reservoirs (snow, soil moisture, groundwater).

1.5 Thesis outline

Studies where gravity is applied in hydrology are twofold: i) local or catchment scale hydrology employing terrestrial gravity, and ii) basin scale hydrology employing satellite geodesy. This thesis is organized according to the same sub-

division. The first part, **Chapters 2–4**, deals with catchment scale hydrology and terrestrial gravity, and the second part, **Chapter 5**, deals with basin scale hydrology and satellite geodesy.

For the first part of the study, data from the Geodynamic Observatory Moxa (Germany), which is located in Silberleite catchment, are employed. **Chapter 2** and **Chapter 3** deal with the detection of hydrological effects on terrestrial gravity. **Chapter 2** describes time series analysis and modeling of gravity, and **Chapter 3** presents an application of a distributed hydrological model to detect hydrological gravity variation. Once the catchment scale hydrological effect on gravity is detected, gravity data are applied in hydrological modeling, which is described in **Chapter 4**.

For the second part of the study, data and models from the Colorado River Basin are employed. In **Chapter 5**, the potential of satellite gravity measurements in basin scale hydrological modeling is investigated, by using spatially distributed estimates of water storage change from GRACE, in combination with hydrological model and in-situ data.

Finally, in **Chapter 6** a general discussion is presented, conclusions are drawn and perspectives for future research are discussed.

Time series analysis and modeling of terrestrial gravity

2.1 Introduction

A time series provides useful information about the system that produced it. Two main goals of time series analysis are: i) identifying the nature of the phenomenon represented by the sequence of observations, and ii) predicting future values of the time series variable or simulating unknown conditions of a system. Both the goals require that some of the system's key properties are determined by quantifying certain features of the time series. These properties can then help better understanding the system and predicting its future behavior. Thus, time series analysis becomes the first step of many investigations.

Detecting change in water storage from related temporal variation in gravity has become an important issue for many studies and research related to the earth and environmental sciences, in particular oceanography, climatology, hydrology and geophysics. Finding the relation between water storage and gravity change is promising for hydrologists, in closing the water balance, as well as for geophysicists, in detecting the real long-term gravity change and improving the signal-to-noise ratio in different frequency ranges.

Although there is a general understanding about the hydrological effect (more qualitative than quantitative) on gravity, until recently gravity has not received much attention from hydrologists. A number of studies have focused on detecting continental and monthly scale water storage change from GRACE

This chapter is an edited version of: Hasan, S., P. A. Troch, J. Boll, and C. Kroner (2006), Modeling the hydrological effect on local gravity at Moxa, Germany, *J. Hydrometeorol.*, 7(3), 346–354, doi:10.1175/JHM488.1.

gravity fields using both synthetic and real data (*Rodell and Famiglietti, 1999, 2001, 2002; Swenson and Wahr, 2002; Swenson et al., 2003; Wahr et al., 2004*), but only a few report on deducing catchment-scale fast responding hydrologic processes from terrestrial gravity observations. Gravity is mostly corrected for hydrological effects by finding and applying empirical relations of different (available) hydrometeorological data (precipitation, soil moisture, groundwater) with gravity residuals (*Mäkinen and Tattari, 1988; Peter et al., 1995; Bower and Courtier, 1998; Crossley and Xu, 1998; Kroner, 2001; Harnisch and Harnisch, 2002*). In this chapter we explore high resolution gravity and hydrometeorological time series to detect causal relationships and evaluate the ability to explain gravity residuals by means of time series modeling.

2.2 Data and methods

The data used in this study are collected at the Geodynamic Observatory Moxa, Germany (Figure 3.1). A detailed description of the study area and data is given in Sections 3.2 and 3.3. In this chapter we used the hourly gravity residuals (for details see Section 3.3.1), precipitation, ground and surface water levels, and temperature (for details see Section 3.3.2).

To explore gravity and hydrometeorological time series to detect causal relationships in our catchment we apply different data analysis techniques on the available time series. Our primary interest is in quantifying gravity variation based on total water storage change in the vicinity of the observatory. In the available hydrometeorological time series, we have two variables that are directly related to water storage: precipitation, representing the hydrological input, and the deep groundwater table, measuring the hydrological state of the catchment.

We apply time series modeling, namely impulse response functions (IRF) to quantify the effect of precipitation on gravity for selected medium to high rainfall events. In contrast to precipitation in the small catchment, the groundwater table is highly variable in space. As a result, the point piezometric level cannot represent the spatial distribution of saturated storage. We therefore apply time series analysis to achieve a qualitative description of the relation between deep groundwater and the observed gravity residual.

2.3 Precipitation and gravity

From visual inspection of the precipitation and gravity residuals (Figure 2.1) it is clear that precipitation has a direct and short-term effect on gravity. Any considerable precipitation event (≈ 5 mm or more) around the observatory causes the gravity signal to drop. Figure 2.1 clearly demonstrates the drop caused by precipitation events, except during the period 6-8 May 2004, when there was a continuous precipitation event. During a continuous event, lasting several days, simultaneous redistribution of water input into the deeper layer would account for a different dynamics in the gravity signal. The drop, observed

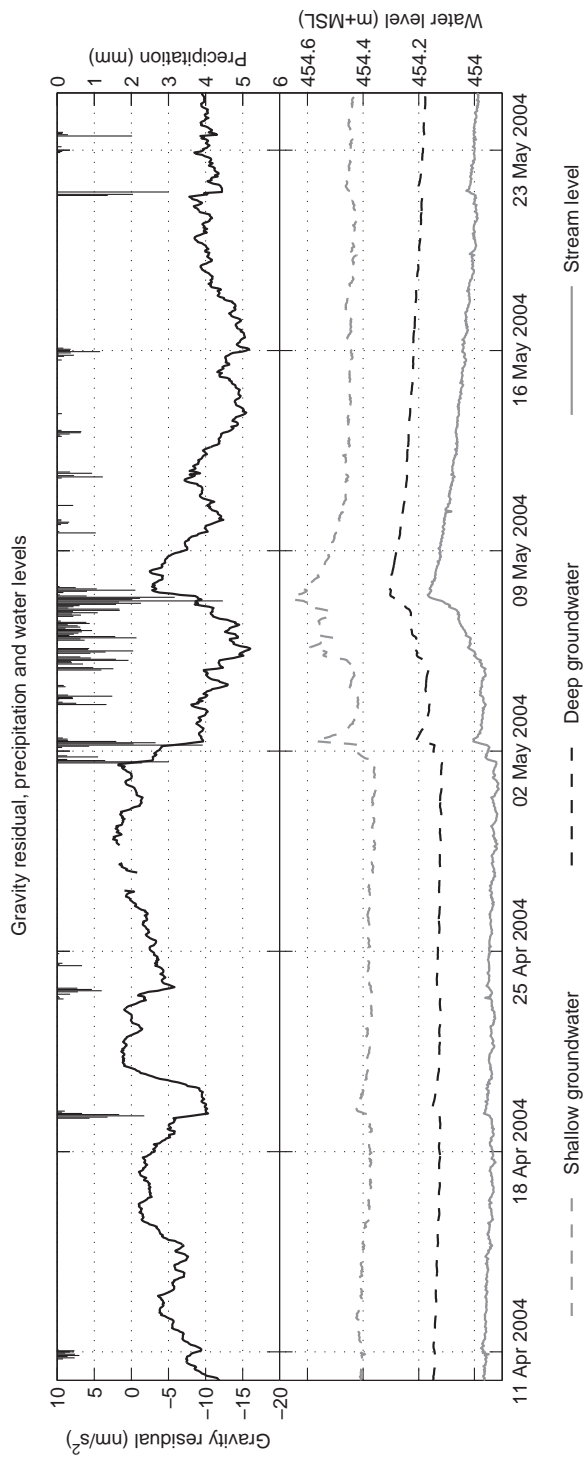


Figure 2.1: Exploring gravity residuals as function of precipitation and water levels (hourly data). Black solid line is for gravity residuals, upper bars for precipitation and lower lines for water levels.

during short isolated events of significant amount, can be explained by the fact that most of the surrounding area is above the gravimeter (Figure 3.1). Any additional mass above the gravimeter will cause the gravity signal to decrease provided rainfall is uniformly distributed over the instrument’s spatial domain.

The short-term effect of precipitation on gravity can be efficiently and accurately modeled by means of linear transfer function models (*Box and Jenkins, 1976*). We consider 4 hour long periods of considerable precipitation (> 8 mm) events isolated by 8 hour long periods of dry spells (maximum precipitation < 1 mm/hour). The above mentioned thresholds of dry and wet periods are selected based on the available data and the selected events are grouped as calibration and validation events.

We compute the impulse response function (IRF) for these selected calibration events, using the z -transform, which is a mathematical operation that, when applied to a sequence of numbers, produces a polynomial function of the variable z . We use a Bayesian information criterion (BIC) (*Priestley, 1981*) that balances model performance and complexity and allows for parsimonious model structure identification. The IRF provides insight into the short-term response of gravity due to rainfall impulses. If $u_{(k)}$ and $y_{(k)}$ denote the input (precipitation in mm during hourly time intervals) and output (gravity changes in nm/s^2 during the same hourly time intervals), the identified transfer function in the z -transform domain can be represented as:

$$y_{(k)} = \frac{-0.33 - 0.42z^{-1} + 0.01z^{-2} + 0.07z^{-3}}{1.00 + 0.61z^{-1}} u_{(k)} \quad (2.1)$$

where z^{-1} indicates the backward shift operator, such that $z^{-1}u_{(k)} = u_{(k-1)}$ and k is a discrete time step counter.

Figure 2.2 shows the identification of the impulse response function, which explains 62% and 57% of the variance of observed gravity change during calibration and validation periods, respectively. The observed and modeled variance are 1.79 and 1.11 during calibration and 1.31 and 0.75 during validation. Figure 2.2a and 2.2d show some selected events along with observed and modeled gravity change during calibration and validation. The IRF demonstrates (Figure 2.2c) the instantaneous drop in gravity caused by a unit precipitation input. The gravity decreases further in the next hour and partially recovers in the following hour. A possible explanation for this recovery is that it mimics the fast hydrological processes in the vicinity of the observatory. After an initial impulse of the rainfall, more or less uniformly distributed around the observatory, redistribution governed by surface and subsurface flow processes allows the gravity signal to recover partially from the immediate drop in magnitude. Our results support our assumption on uniform rainfall distribution, otherwise we would not find that the linear transfer function model would be able to explain gravity changes for different rain events in a very similar way.

Explaining the gravity residuals by means of the impulse response function is valid only for short-term gravity changes that occur because of a precipitation impulse. A precipitation event can also mean a water mass loading on the

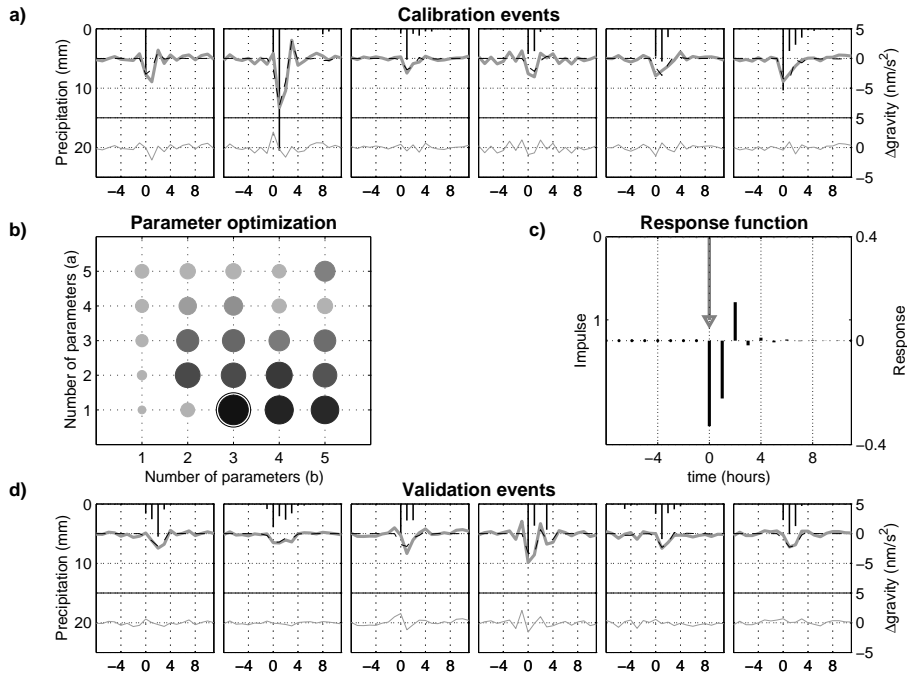


Figure 2.2: Short-term gravity response to rainfall impulses. a) Model calibration showing selected precipitation events (vertical bars) along with observed (thick gray line) and modeled (dashed line) changes in gravity residuals (top) and model error (thin gray line at bottom). b) Model structure characterization: a and b represent number of parameters in autoregressive and moving average polynomials of the transfer function. Size and shade of the circles represents values of $-\text{BIC}$. The optimized value is marked by a circle ($b = 3, a = 1$). c) Optimized unit impulse (arrow showing precipitation) response (black bars showing gravity change) function. d) Model validation showing selected precipitation events (vertical bars) along with observed (thick gray line) and modeled (dashed line) changes in gravity residuals (top) and model error (thin gray line at bottom).

surface. The loading effect of local (area of few km²) water masses on gravity is negligible, as it is on the sub nm/s² scale and not detectable by the gravimeter. The IRF does not account for redistribution or loss of water in the catchment at larger time scales (days). For long-term gravity changes we need to look at the storage changes induced by redistribution of available water in the subsurface. Our next step is exploring gravity with deep groundwater, which represents, to some extent, the available storage of the catchment at a given moment in time.

2.4 Groundwater and gravity

Unlike precipitation effects on gravity, the effect of groundwater change is less trivial. Both the deep and shallow piezometers react instantaneously to precipitation and coincide with the quick water level changes in the stream (Figure 2.1). From this observation we can conclude that both the deep and shallow aquifers are well connected to the stream that drains the area surrounding the gravimeter and excludes the possibility of a confined groundwater system. As discharge (flux) is proportional to available water storage (state), the deep or shallow groundwater store represents the water storage condition of the catchment. Although the groundwater table measured at a point is indicative for the available water storage, we do not have much information about the spatial distribution of groundwater storage due to lack of distributed observations and detailed hydro-geological information. In our subsequent analysis we consider deep groundwater data only, as we have longer time series available for this variable.

Gravity, being an integrated signal, contains information related to all kinds of simultaneous mass (re-)distributions. Thus, similar changes in groundwater storage do not necessarily cause similar gravity changes. Depending on other (e.g. soil moisture) storage conditions, gravity change can be different for equal groundwater variation. As a result, we should not expect a unique relation between groundwater and gravity. We calculated the moving-window cross-correlation between groundwater and gravity with windows of varying length (from 1 day to 1 month) at a 0 to 5 hour lag. Looking at the histograms of the cross-correlation coefficients, we find both positive and negative high correlation, as well as no correlation (Figure 2.3a).

In more than 50% of the cases there exists a high negative correlation ($\rho < -0.6$) between deep groundwater and gravity. The deep groundwater normally has a negative correlation with gravity because it is highly correlated with near surface water storages (soil moisture, etc), which have more mass variability than deep groundwater and generally lay above the gravimeter in the area. The high positive correlation or no correlation demonstrates a seasonal pattern. It is mainly during winter months (November - February) that we see either high positive correlation or no correlation at all. We looked at the average hydrometeorological conditions (groundwater, temperature, precipitation) of the cross-correlation windows (Figure 2.3b, 2.3c). At the time of high positive correlation or no correlation, average temperature is lower. A possible

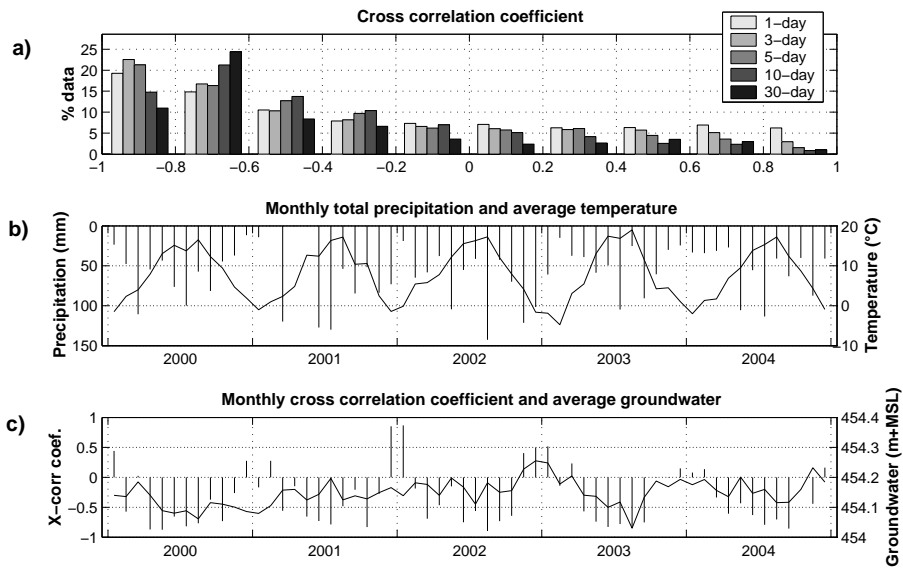


Figure 2.3: Exploring groundwater and gravity. a) Windowed lag-0 cross-correlation between groundwater and gravity for windows of different time lengths. b) Monthly average precipitation (bars) and temperature (line). c) Monthly correlation between groundwater and gravity residual (bars) and average groundwater table (line).

explanation for the high positive correlation during cold periods could be related to different dynamics in the soil moisture caused by freezing of the upper soil layer or by the vegetation using less water from the soil moisture. A frozen layer would decrease the evapotranspiration and slow down the redistribution processes. As the rate of transpiration is influenced by factors such as humidity and temperature, during cold (low temperature) and wet (high humidity) winter months there would be much less transpiration from the spruce trees in the catchment. As a result, water uptake from the soil moisture would be considerably lower, making the soil moisture storage less dynamic. Thus, when freezing temperatures limit soil moisture changes, variations in deep groundwater storage, which generally lays below the gravimeter in the area, dominate the mass (gravity) signal.

2.5 Discussion

In this chapter, time series analysis is explored to explain local gravity variation as observed by a superconducting gravimeter. This approach yields encouraging results and confirms why gravity is mostly corrected for hydrological effects by finding and applying empirical relations of different (available) hydrometeorological data (precipitation, soil moisture, groundwater) with gravity residuals. Time series modeling provides us with a simple yet effective technique to correct for precipitation effects on short-term gravity residuals. Analysis of deep groundwater and gravity residuals demonstrates different dynamics present in the catchment.

Time series analysis is mostly done in both the time and the frequency domain. In our case, we have done this analysis only in the time domain, mainly because of the following reasons. Measured gravity (or its temporal variation) contains effects of many periodic components of different frequency and magnitude, as discussed in Chapter 1. Hydrometeorological variables also contain some periodicities. In order to obtain the gravity residuals, the raw signal has to be filtered out. As a result, frequency domain analyses are already performed in the process of obtaining the gravity residuals.

The time series analysis described above does not directly consider any gravity change induced by hydrological processes. In order to account for hydrological processes acting in our catchment, we need to apply hydrological models to model gravity changes. The next chapter deals with the application of a distributed hydrological model to compute gravity variation.

Distributed hydrology to model terrestrial gravity variation

3.1 Introduction

Classical distributed catchment-scale hydrological models that have been optimized for use with sparse in-situ observations are often inappropriate for exploiting remote sensing data and thus have to be extended or significantly rethought and reformulated (*Troch et al.*, 2003a). For any given catchment-scale, the relation between gravity variation and storage (mass) change in principle should be the same. Incorporating data on gravity variation in catchment-scale hydrological modeling can greatly enhance our understanding of flow and storage processes and may lead to improved data assimilation techniques, for instance, by constraining water balance fluctuations. However, to quantify the hydrological effect on terrestrial gravity variation, we need a sound hydrological model that simulates distributed storage conditions.

As mentioned earlier, gravity is mostly corrected for hydrological effects by finding and applying empirical relations of different (available) hydrometeorological data (precipitation, soil moisture, groundwater) with gravity residuals. In doing so, the hydrological processes responsible for redistribution of water storage are generally ignored or strongly simplified.

Here we evaluate the ability to explain gravity residuals by means of distributed hydrological modeling. Our primary interest is in quantifying gravity

This chapter is an edited version of: Hasan, S., P. A. Troch, J. Boll, and C. Kroner (2006), Modeling the hydrological effect on local gravity at Moxa, Germany, *J. Hydrometeorol.*, 7(3), 346–354, doi:10.1175/JHM488.1.

variation based on total water storage change in the vicinity of the observatory. To evaluate the ability to explain gravity residuals by means of distributed hydrological modeling we apply the Soil Moisture Routing (SMR) model (*Boll et al.*, 1998) to track temporal changes in near surface storage in the catchment around the gravimeter. We then compute the gravity variation caused by water storage change in the unsaturated zone using Newton’s law of gravitation in a local Cartesian coordinate system.

3.2 Study area

The Global Geodynamics Project (GGP) (*Crossley et al.*, 1999) began in 1997. One of the purposes was to record the earth’s gravity field with extremely high accuracy (temporal variation with an accuracy of $\sim 10^{-9}$ m s $^{-2}$) at a number of stations around the world using superconducting gravimeters (SGs). Each site is visited at least twice per year with an absolute gravimeter to co-determine secular changes and to check calibration. The SG data are being used in an extensive set of studies of the earth, ranging from global motions of the whole earth to the gravity effects of atmospheric pressure and terrestrial water storage. The SG stations are run independently by national groups of scientists. For our study we use data from the Geodynamic Observatory Moxa (one of the GGP stations), Germany.

3.2.1 Location and background

The Geodynamic Observatory Moxa (established in 1964) has a tradition of more than 50 years of seismological observations. The village of Moxa is in the Federal state of Thuringia in Germany (Figure 3.1, geographic coordinates are 50.6447 N, 11.6156 E and altitude is 455 m above mean sea level). The observatory, located in the Silberleite valley, is near the Thuringian slate mountains. The site of Moxa was chosen because it was close enough to Jena (about 30 km south), but at the same time sufficiently far away from industrial plants, major roads, and towns. The given criterium was that none of those should exist within a radius of 10 km. Another decisive factor was the existence of the Silberleite valley, which allowed building the observatory partly into a hill, in order to reduce noise caused by industrial plants, major roads, towns and to enhance temperature stabilization. Having stable bed rock and other necessary environmental conditions for installation of sensitive geophysical instruments (*Teupser*, 1975), the valley hosts the Geodynamic Observatory Moxa (one of the German GGP stations). During the years 1996 to 1999, the seismological station was modernized and extended into a geodynamic broadband observatory. Its general objective is to monitor, analyze, and interpret geodynamic signals due to the mass shifts and deformations at the earth’s surface ranging from seismic frequencies up to long-term variations. With the establishment of GGP in 1997, the research interest of the observatory was extended to finding the hydrometeorological effect on geophysical data.

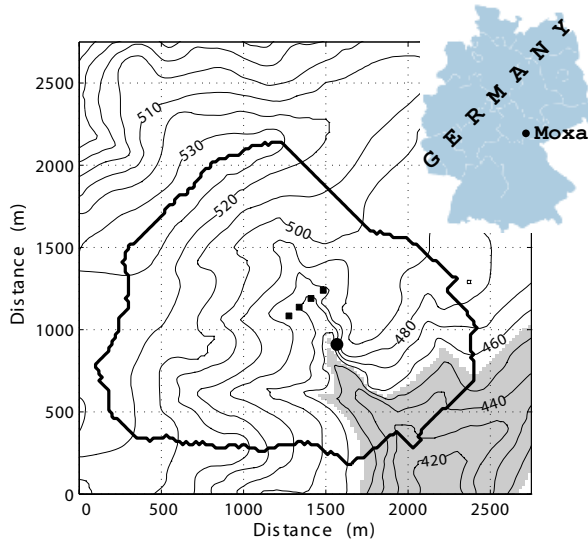


Figure 3.1: Location (top-right) and topography (distances are in m, elevations are in m+MSL, contour interval is 10 m) of Silberleite catchment (thick line is the catchment boundary) of Moxa, Germany. The shaded area is lower than the elevation of the gravimeter. The large dot shows the location of the gravimeter, the weather station, a V-Notch and piezometer for groundwater. The small squares show locations (upstream of V-Notch), where ground and surface water levels are monitored.

3.2.2 Geophysical characteristics

The observatory (Silberleite catchment) is situated in a spruce forest and the surrounding mountains consist of intensively folded and fractured basement rocks. In the surroundings of the station thick series of slates and graywackes of Paleozoic (lower and upper Visean) Age are found. The elevation in the catchment varies between 425 and 535 m+MSL. Most of the surrounding area within the catchment is above the gravimeter (Figure 3.1). The hillslopes present in the catchment are of various shapes, gradients and characteristics. Field investigations show the presence of many preferential flow paths under the soil cover caused by secondary porosity in folded and fractured bed rock (shales). The Silberleite valley at the observatory is a second Strahler order catchment with intermittent and ephemeral streams. The main runoff generation processes are saturation excess runoff in the riparian zone and rapid snowmelt. The soil layer (including the weathering layer) has mostly a depth between 0.4 and 1.0 m.

3.2.3 Hydrometeorological characteristics

Thuringia is located in a region in which maritime wet and continental dry influences practically balance. A main factor regarding the climate are the low mountain ranges. The mean annual temperature is 7.5°C , where January is the coldest month (mean temperature of -1.5°C) and August the warmest (mean temperature of 16.5°C). The average annual precipitation is approximately 700 mm, with mean monthly precipitation ranging between 30 and 85 mm.

3.3 Data

3.3.1 Gravity

The hourly gravity residuals, hereafter referred to as observed gravity residuals, are derived by filtering and reducing for earth tides, polar motion, barometric pressure variations, and instrumental drift. Figure 3.2 illustrates the order of magnitude of temporal gravity changes caused by the two main components, earth tides and barometric pressure. Continuously varying components are normally calculated in nm s^{-2} from station parameters, while the long-term component of the data set is removed by adjusting and subtracting a linear drift. More information about site specific gravity reduction can be found in *Kroner et al.* (2004). The gravity residuals still contain effects of an earthquake (around 05 May 2000 in Figure 3.2), which is visible as a high frequency perturbation that lasted for a short period.

3.3.2 Hydrometeorology

The hydrometeorological data in the vicinity of the observatory (large dot in Figure 3.1) include hourly precipitation, groundwater (filter at 48 m below the

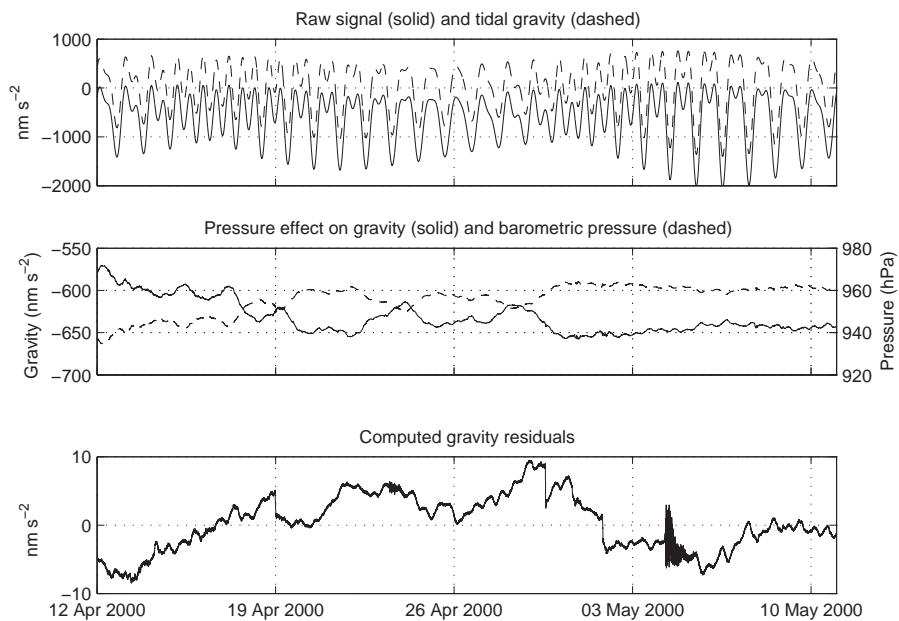


Figure 3.2: Gravity reductions applied to the raw gravity signal at a 1 minute time step.

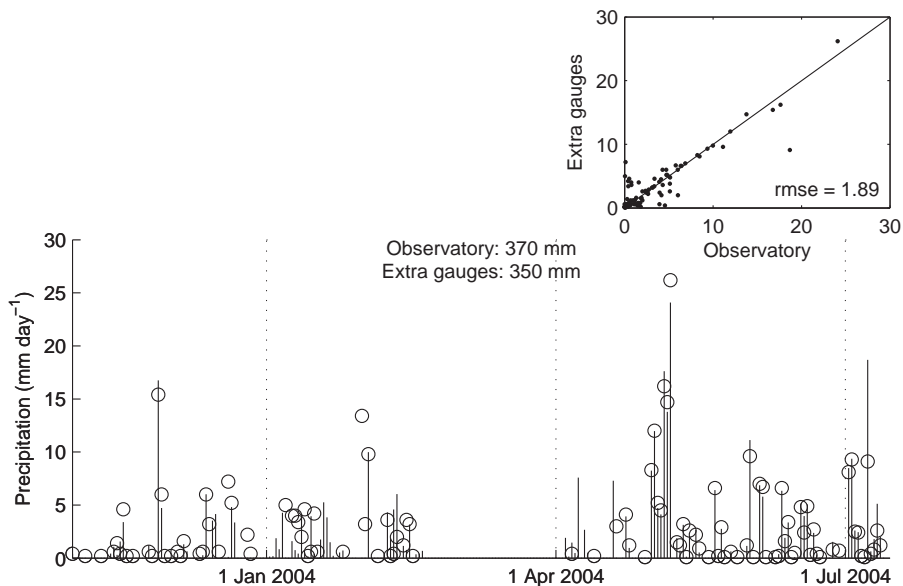


Figure 3.3: Comparison of precipitation data from different rain gauges. Bars show the data from the observatory and circles show the average of extra rain gauges. Inset: scatter plot between the two variables.

land surface), barometric pressure, temperature, wind speed, humidity, and illuminance. Moreover, we have occasionally sampled surface water levels at and discharge through a V-Notch installed in the Silberleite near the observatory. The above mentioned data collection started during the second half of 1999. At the end of 2003, additional piezometers were installed near the observatory and at a section (small squares in Figure 3.1) upstream of the V-Notch at a depth ranging between 1 and 2 m to monitor the shallow (near-surface) groundwater table (in the riparian area), together with an automatic water level recorder upstream of the V-Notch. Two additional rain gauges to check spatial variation in precipitation, and a solarimeter to convert the illuminance data for estimation of net radiation, were also included in the new data collection program. In the following paragraphs, we will briefly discuss the data collected, converted and used for our study of terrestrial gravity variation.

Precipitation: As we are dealing with a small catchment ($\approx 3 \text{ km}^2$), we consider the point precipitation to be uniformly distributed over the whole catchment. This assumption is supported by the nature of most storms in the area, being generated by frontal systems with spatial scales much larger than our catchment. However, this assumption was also checked by using data from additional rain gauges (Figure 3.3), installed temporarily. A reason for total underestimation and temporal overestimation of precipitation by those

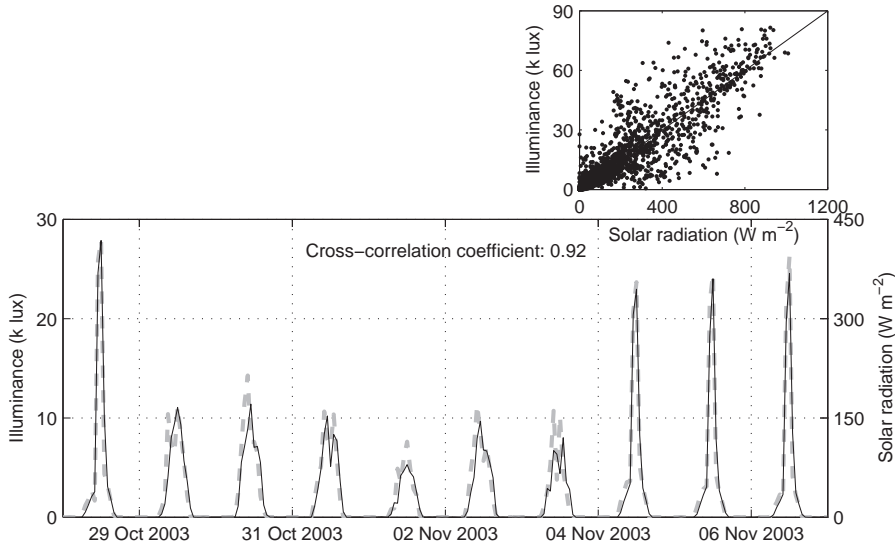


Figure 3.4: Conversion of illuminance data to solar radiation: gray dashed line shows the recorded illuminance and black solid line shows solar radiation. Inset: scatter plot between the two variables.

rain gauges is that those suffered from dirt (leaves, insects) being collected/accumulated in the rain gauges.

Solar radiation: We estimated solar radiation converted from illuminance data, which is not very common in hydrological measurement systems. Illuminance is the total amount of visible light illuminating a point on a surface from all directions above the surface. Therefore illuminance is equivalent to irradiance weighted by the response curve of the human eye. The ratio between illumination and radiation intensity can vary with solar zenith distance (*List, 1968; Kimball, 1924*). However, comparing solar radiation data from a recently installed solarimeter next to the existing illuminance meter, we found good agreement (cross-correlation coefficient of 0.92) between illuminance and solar radiation (see Figure 3.4).

Discharge: The discharge data used in our study are from occasionally sampled surface water levels at and discharge through a V-Notch installed in the Silberleite. Because of hydraulically improper design and construction, the V-Notch is neither a broad nor a sharp crested weir. However, we constructed a replica of the existing weir in the laboratory. Based on available data and current instrumentation information, we estimated the relationship between upstream water level and discharge through the V-Notch (Figure 3.5).

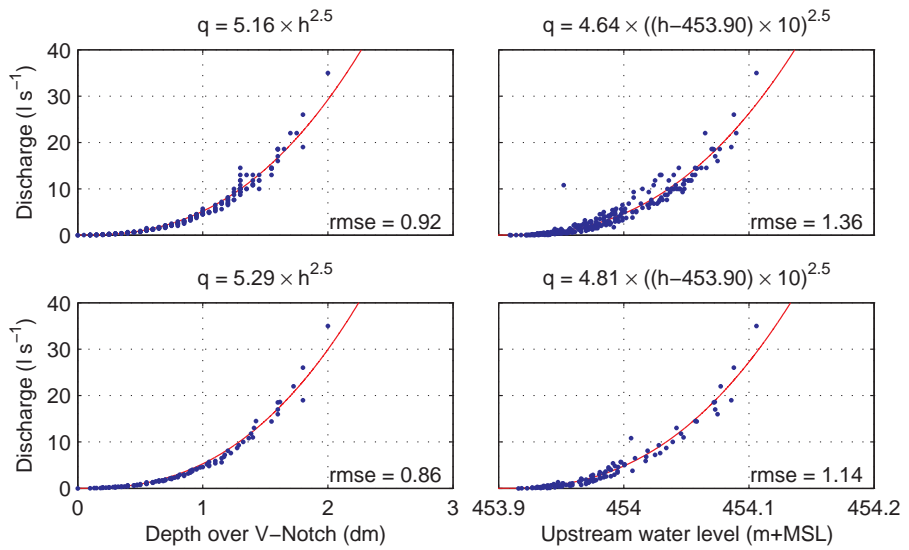


Figure 3.5: Stage-discharge relation of an existing V-Notch in Moxa catchment. Water levels in the left hand graphs were collected manually, while the data in the right hand graphs are from an automatic water level recorder. The top graphs represent all available data, while the data in the bottom graphs are for average data. The root mean square errors are given in the right bottom corner of each plot.

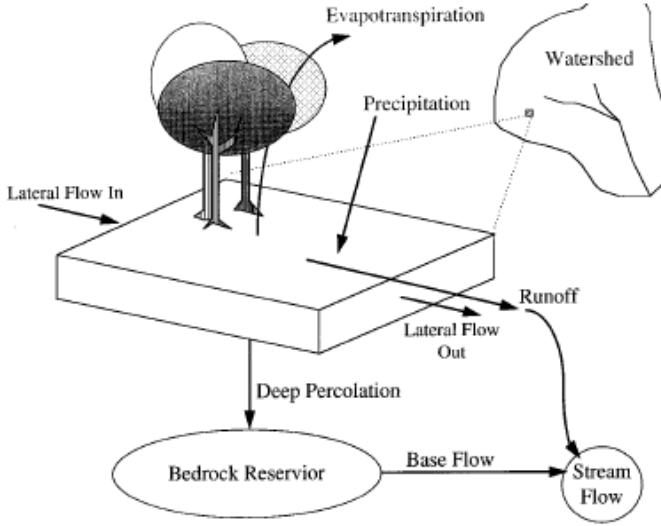


Figure 3.6: Soil Moisture Routing (SMR) model concept (*Frankenberger et al., 1999*).

3.3.3 Auxiliary data

A Digital Elevation Model (DEM) of 20 m resolution covers an area of 4 km radius around the observatory. Other than the topography, we do not have detailed information regarding spatial heterogeneity (e.g. soils) of the catchment. However, soil samples were collected and laboratory tests of those samples were made to determine soil properties, used in hydrological modeling. The laboratory tests were determination of soil porosity, moisture contents at field capacity and wilting point, residual moisture content, and saturated hydraulic conductivity.

3.4 Soil Moisture Routing (SMR) model

The Soil Moisture Routing (SMR) model (*Boll et al., 1998; Frankenberger et al., 1999*) provides distributed predictions of surface runoff and soil moisture and keeps track of interception store and storage in snow cover. The model tracks the flow in and out of grid cells of the soil layer using a basic mass balance:

$$D_i \frac{d\theta_i}{dt} = P - ET_i + \sum Q_{in.i} - \sum Q_{out.i} - L_i - R_i \quad (3.1)$$

where, i is cell address, D_i is depth to restrictive layer of the cell, θ_i is average soil moisture content of the cell, P is precipitation (throughfall and snowmelt),

ET_i is actual evapotranspiration, $Q_{in.i}$ is lateral inflow from neighboring upslope cells, $Q_{out.i}$ is lateral outflow to neighboring downslope cells, L_i is downward leakage to bedrock (percolation), and R_i is surface runoff. Note that all the volumetric quantities are presented per area of a grid cell.

Calculation of the water balance is facilitated by a GIS, which keeps track of catchment characteristics such as elevation, soil properties, slope, land use and flow direction as well as the moisture stored in each cell at each time step. In this study, the modeling time step is one hour. Although the land use is mainly spruce forest, we distinguish the observatory area and the riparian zone from the main land use type. Being closest to the gravimeter, the observatory area has the biggest effect on gravity and that needs to be modeled carefully. The area ($\approx 100 \times 100 \text{ m}^2$) around the observatory does not have trees and the roof over the gravimeter has a soil depth of 2.5 m with higher rock percentage. The riparian zone is modeled with less porosity in order to facilitate more surface runoff than that of average soil cover. Modifications to the original SMR model include the addition of a canopy layer to simulate interception, and calculation of gravity variation based on moisture storage in the canopy, snow and soil.

Based on Newton's law of gravitation in a local Cartesian coordinate system, the vertical component of gravitation (gravity anomaly) at location r due to a disturbing mass at location r' is computed by

$$\Delta g(r) = G \iiint_v \frac{\Delta \rho(r')(z' - z)}{|r' - r|^3} dv \quad (3.2)$$

with the density difference $\Delta \rho$ of the disturbing mass relative to its surroundings, and the volume element $dv = dx' dy' dz'$.

Closed-form solutions of Equation 3.2 are available for a multitude of simple bodies with constant density (*Torge, 1989*). We used rectangular prisms (*Nagy, 1966*) with horizontal limits defined by the pixel size in the DEM ($20 \times 20 \text{ m}^2$) and vertical limits of soil depth for soil moisture, snow depth for the snow layer, and canopy interception storage depth for the canopy layer.

3.5 Analysis and results

The SMR model for the Silberleite catchment was set up from available data sets (DEM, land use, and soil depths). Proper model calibration was hampered because of lack of good quality runoff data. We checked the SMR model results for consistency in computed water balance components and estimated monthly runoff. In general, the model water balance is in agreement, for example, with estimates of the evaporation/precipitation ratio of 0.5 (*Peixoto and Oort, 1992*). Monthly runoff was estimated from available surface water level data and compared to modeled monthly runoff. While judging this verification, we have to keep in mind that no data were collected during high discharge and the fact that our model does not have a deep groundwater component, therefore, the regional base flow contribution to the total runoff at the weir

is not simulated. However, the simulated runoff pattern was more or less in agreement with the observed flow pattern.

Figure 3.7a, b compares the observed gravity residuals for a 4-year period (April 2000 - May 2004) with the modeled gravity changes based on spatio-temporal simulations of the water balance components in the catchment. We model the change in gravity, which is then cumulated to a gravity residual. The observed gravity residual has a number of data gaps and it cannot be claimed that the residuals are only due to hydrological changes. In comparing the observed gravity residuals and modeled gravity variation, our focus is mainly on the dynamic pattern of the signals. In general, we can reproduce the observed patterns quite well, although the dynamic range of modeled gravity variation is about 50% of the observed gravity residuals. One possible reason could be that the modeled influence zone of mass distribution around the gravimeter underestimates the true influence zone, due to the fact that groundwater dynamics are poorly represented in the hydrological model. If we check the range of gravity variation caused by maximum soil moisture variability (difference between dry and saturated soil condition in the catchment), we find that the soil moisture variability alone cannot explain the observed gravity variation.

Figure 3.8a shows the effect of the domain size considered in gravity calculation. For calculation of gravity variation, storage change in each pixel of the total catchment was considered. In order to analyze the effect of the domain size, we considered circular domains of different radius around the gravimeter. From Figure 3.8a it becomes clear that the domain of the total catchment and of the circle of 600 m radius ($\approx 40\%$ of the total catchment) around the gravimeter show the same dynamic range of gravity variation.

Figure 3.8b shows the effect of the different components (soil moisture, snow and canopy storage) considered in the gravity calculation. As expected, changes in canopy storage do not have much influence on changing gravity. During cold periods, gravity variation due to changes in soil moisture storage are rather low, compared to changes in snow storage. Including the effect of gravity variation due to changes in snow storage does significantly improve our model.

Although the general pattern of observed residuals and modeled variation are in good agreement, we experience some periods where modeled variations do not follow the pattern of observed residuals. The time periods during which the modeled gravity variations do not follow the observed pattern are mainly the winter months (November - February). During the winter months we can expect different dynamics in the saturated and unsaturated zones. In the time series analysis (Chapter 2) we have seen a high positive correlation between the deep groundwater and gravity residuals during the same winter months, when modeled variation does not follow the observed pattern. The SMR model confirms less dynamics in the unsaturated zone during the winter months, when relation between deep groundwater and gravity residuals switches from a negative to a positive or no correlation (Section 2.4).

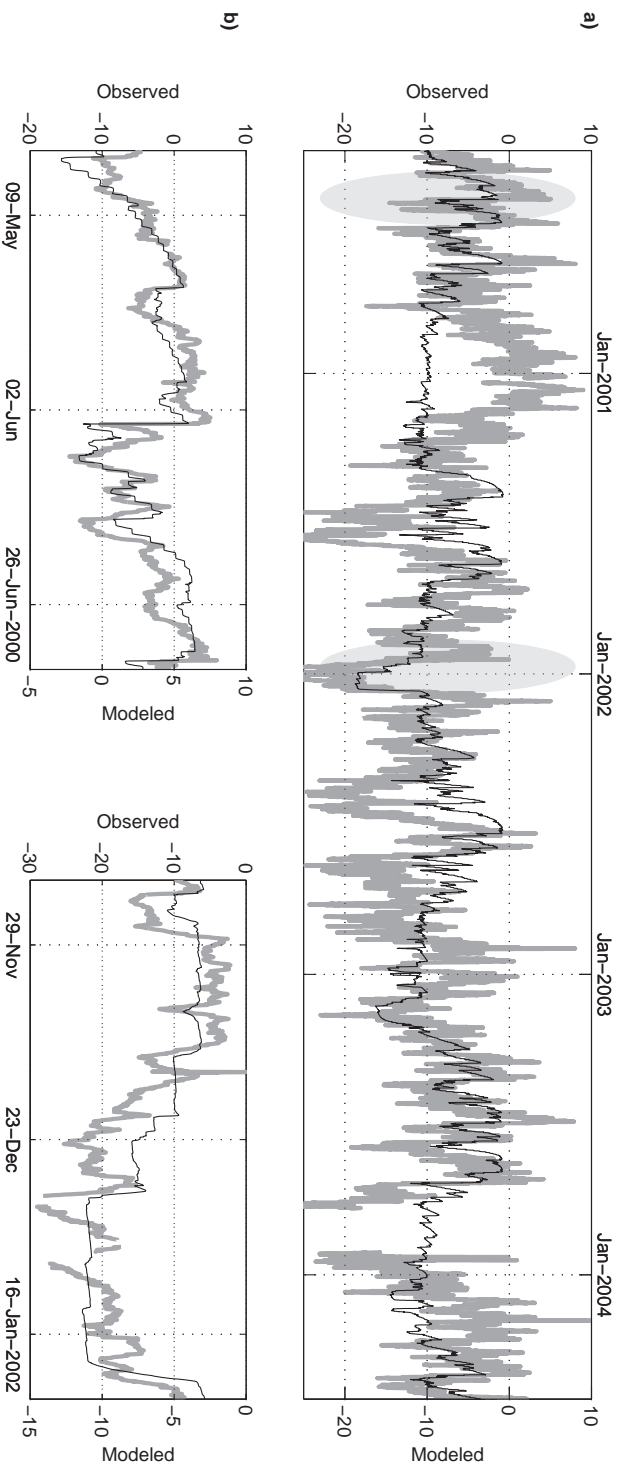


Figure 3.7: Modeling gravity variation: a) Observed (gray) and modeled (black) gravity variation. Model includes gravity variation due to soil moisture, snow and canopy storage. Shaded areas are zoomed in and shown in b. b) Zoomed version of a. Note different scales for observed and modeled variation in a, and b.

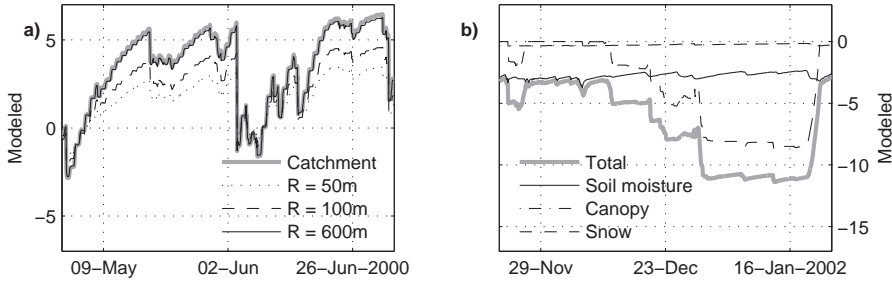


Figure 3.8: Modeling gravity variation: a) Effects of different domains in a small time window. R is domain radius. b) Effects of different components in a small time window. Note different scales for observed and modeled variation in *a*, and *b*.

3.6 Discussion

The availability of digital geographic data, particularly digital elevation models, makes distributed hydrological modeling possible. At the same time, surface heterogeneity and the lack of subsurface data makes the modeling difficult. SMR was developed specifically for topographically steep areas, hydrologically characterized by relatively thin, permeable soil layers over a much less permeable fragipan, bedrock, or other restricting layer. The model is most effective where slopes are steep enough to be the main cause of lateral flow. SMR application is limited to regions fitting the description discussed above and should not be viewed as a general or universal hydrology model.

In this chapter, a distributed hydrological modeling technique was explored to explain local gravity variations as observed by a superconducting gravimeter. Distributed water balance modeling explains both short and long-term behavior of the gravity signal. The hydrological model confirms the findings of our time series analysis (Chapter 2).

The periods (winter months: November - February) of high positive correlation between groundwater and gravity changes (Chapter 2) coincide with the periods where modeled gravity variations do not behave as observed gravity residuals. This study shows that the application of a distributed hydrological model can be useful in modeling gravity residuals. More hydrogeological and geophysical investigations are needed to extend the existing model.

Application of terrestrial gravity variation in hydrological modeling

4.1 Introduction

The central problem in catchment hydrology is to accurately measure and model atmospheric forcing and hydrologic partitioning at large spatial scales. The issue is complicated as most observations of hydrometeorological fluxes (e.g. precipitation, evaporation) and subsurface storage (e.g. soil moisture, phreatic groundwater level) are available only at the point-scale. Landscape heterogeneity (topography, soils, vegetation) and space-time variability of atmospheric forcing prevent simple upscaling to catchment relevant stores and fluxes. However, much progress has been made recently using remotely sensed information to develop spatial estimation methods for precipitation (e.g. *Krajewski et al.* (2006); *Bales et al.* (2006)), evaporation (e.g. *Bastiaanssen et al.* (1997); *Su* (2002)), soil moisture (e.g. *Su et al.* (1997); *Verhoest et al.* (1998); *Njoku and Li* (1999); *Jackson et al.* (1999)), stream flow (e.g. *Alsdorf and Lettenmaier* (2003)), and terrestrial water storage (e.g. *Rodell and Famiglietti* (1999, 2001, 2002)). Application of several of these advanced observation methods to smaller catchments (hereafter defined as the intermediate scale: 10^0 to 10^1 km²) is difficult due to spatial and temporal resolution limits of the required satellite data. Developments of geophysical measurement techniques

This chapter is an edited version of: Hasan, S., P. A. Troch, P. W. Bo-gaart, and C. Kroner (2008), Evaluating catchment-scale hydrological modeling by means of terrestrial gravity observations, *Water Resour. Res.*, 44, W08416, doi:10.1029/2007WR006321.

(e.g. ground penetrating radar, electrical resistivity tomography, electromagnetic induction) pave the way towards progress in observing hydrologic state variables and fluxes at this intermediate catchment-scale. Recent progress in accurately monitoring temporal gravity variations by means of superconducting gravimeters is another addition to the geophysical measurement techniques.

It is estimated that hydrometeorological variations (e.g. water storage, atmospheric pressure) can cause ~ 5 to 100 nm s^{-2} changes in gravity at a daily to yearly time scale (*Torge, 1989*). Several studies have investigated empirical relationships between hydrometeorological and gravity data (*Mäkinen and Tattari (1988); Peter et al. (1995); Bower and Courtier (1998); Crossley and Xu (1998); Kroner (2001); Harnisch and Harnisch (2002); Van Camp et al. (2006)*). Very few studies have used hydrological modeling to explain local, regional and continental hydrological effects on gravity (*Hasan et al. (2006); Van Camp et al. (2006); Hinderer et al. (2006)*). *Pool and Eychaner (1995)* and *Pool (2005)* show that temporal variations in gravity, determined by repeated gravity surveys, can be used to estimate aquifer storage change.

In the previous chapters we showed applications of time series analysis and distributed hydrological modeling techniques to understand the effect of the hydrological processes on observed gravity residuals. In this chapter we investigate how observed gravity residuals can aid catchment-scale hydrological modeling. Considering gravity observations as an integrator of catchment-scale hydrological response (similar in nature as discharge measurements), we use gravity variation data to constrain hydrological models of the catchment. We use a simple lumped water balance model to model soil moisture and snow storage change and a semi-distributed hydraulic groundwater model (*Troch et al., 2003b*) to model hydrological processes in the catchment. The temporal change in gravity is calculated using the distributed storage information of different components. To calibrate the models we used both discharge and gravity data.

4.2 Modeling approach

We hypothesize process-based links between hydrological change and gravity variation, and built our models accordingly. Based on the time scale of hydrological processes, we group water storage changes into i) fast and ii) slow storage change, calculated for hourly and daily time-steps respectively. The fast storage change process includes changes in root zone water content caused by precipitation, and changes in snow storage caused by snowfall and snowmelt. The slow storage change process includes water losses in root zone water storage through evapotranspiration and recharge, redistribution in saturated water storage, and discharge.

In line with the above mentioned groups of hydrological processes, we classify the temporal gravity variation into:

1. Fast (e.g. hourly) gravity variation caused by precipitation, and
2. Slow (e.g. daily) gravity variation caused by subsurface water redistribu-

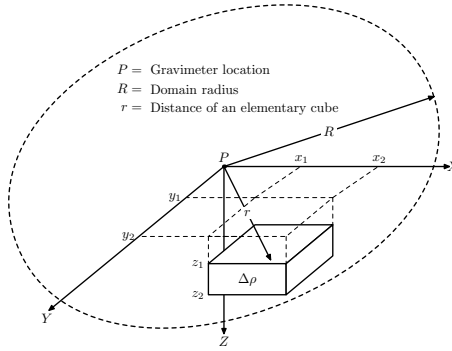


Figure 4.1: Sketch illustrating modeling of gravity variation from storage changes.

tion.

To model gravity variation, we need distributed information of mass (density) change. A distributed hydrological model is the logical tool to compute temporal gravity variation for different water storage changes. However, we do not have detailed information regarding spatial heterogeneity (e.g. soils) of the catchment except for its topography. In the previous chapter, we found negligible subsurface (unsaturated) lateral flow and insignificant gravity variation due to canopy storage change. Thus a simple lumped water balance model for surface (snow) and near-surface (soil moisture) storage dynamics was chosen. Results from the lumped water balance model are then re-distributed in the catchment using topographic information. Regarding saturated water storage dynamics, we divided the catchment into several hillslopes, based on topography. Thus a semi-distributed hydraulic groundwater model for saturated storage and fluxes could be built.

4.2.1 Gravity model

Once the gravity residuals are derived, the remaining variation is primarily caused by mass changes of hydrological nature. Based on Newton's law of gravitation in a local Cartesian coordinate system, the vertical component of gravitation (gravity anomaly) at location $p(x, y, z)$ due to a disturbing mass at location $p'(x', y', z')$ is computed by:

$$\Delta g(p) = G \iiint_v \frac{\Delta \rho(p')(z' - z)}{|p' - p|^3} dv \quad (4.1)$$

where $\Delta \rho$ is the density difference of the disturbing mass relative to its surrounding, the volume element $dv = dx'dy'dz'$ and the gravitation constant $G = 6.673 \times 10^{-11} \text{ m}^3 \text{ kg}^{-1} \text{ s}^{-2}$.

Closed-form solutions of Equation 4.1 are available for simple bodies with constant density. For an elementary cube with the limits $x_1, x_2, y_1, y_2, z_1, z_2$

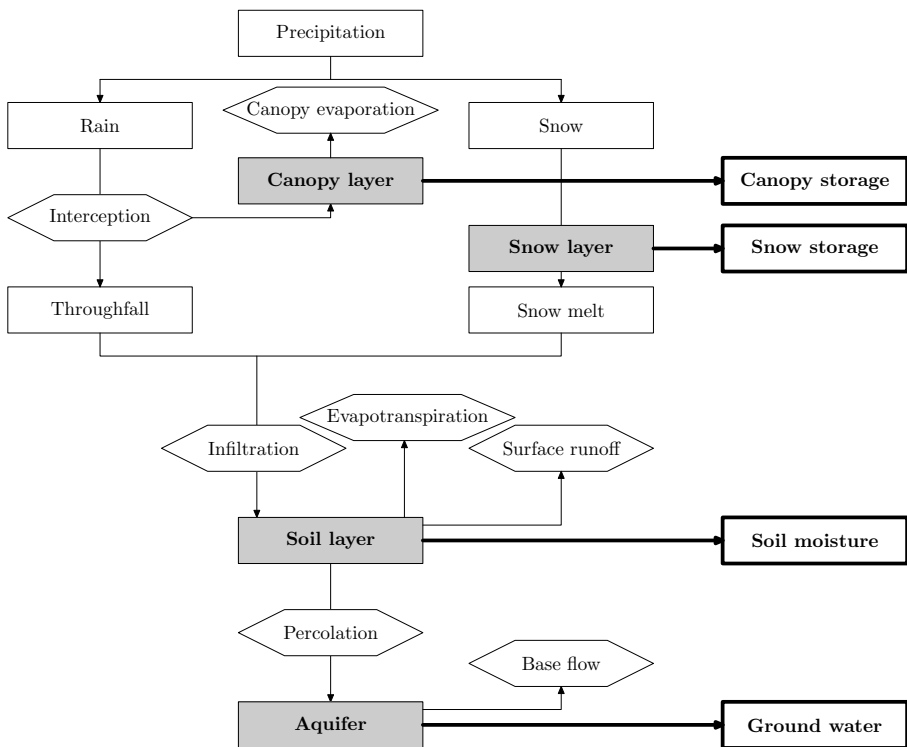


Figure 4.2: Schematic illustrating relevant hydrological processes considered in the models used.

(Figure 4.1) we have (Nagy, 1966):

$$\Delta g(r) = G\Delta\rho \left[\left[\left[c - x \ln(y+r) - y \ln(x+r) \right. \right. \right. \quad (4.2)$$

$$\left. \left. \left. + z \arctan \frac{xy}{zr} \right]_{x_1}^{x_2} \right]_{y_1}^{y_2} \right]_{z_1}^{z_2}$$

with $r = \sqrt{x^2 + y^2 + z^2}$. Equation 4.2 is the basis for all calculation of gravity variation. For any storage change, distributed computations of gravity variations are summed up, for the considered domain, to calculate the total gravity variation at the gravimeter location.

4.2.2 Hydrological model

Modeling of hydrological storage and fluxes is done in two steps. First, we use a lumped water balance model that provides average soil moisture and snow storage conditions. Second, we use the hillslope-storage Boussinesq (hsB) model (Troch *et al.*, 2003b) that provides semi-distributed saturated water storage conditions in the catchment. Figure 4.2 illustrates the processes considered

in our hydrological models. The storage dynamics modeled are then used to calculate changes in gravity.

Lumped water balance model

The lumped water balance model basically keeps track of hydrological stores and fluxes (shown in Figure 4.2) in the unsaturated zone and snowpack.

The balance equation for the unsaturated zone is:

$$L \frac{d\theta}{dt} = P - E - N - R \quad (4.3)$$

where L is depth of the unsaturated zone (cm), θ is average soil moisture content ($\text{m}^3 \text{ m}^{-3}$), t is the time step (hr), P , E , N and R are rates of precipitation (throughfall and snowmelt) (cm hr^{-1}), actual evapotranspiration (cm hr^{-1}), downward leakage (drainage) (cm hr^{-1}) to bedrock, and surface runoff (fraction of throughfall and snowmelt) (cm hr^{-1}) respectively.

The balance equation for the snowpack is:

$$\frac{dS_{sn}}{dt} = P_{sn} - M \quad (4.4)$$

where S_{sn} is depth of snow water equivalent (cm), t is the time step (hr), P_{sn} and M are rates of snowfall (cm hr^{-1}) and snowmelt (cm hr^{-1}), both in water equivalent.

Precipitation is classified as rain or snow based on a threshold temperature. Part of the rain is intercepted by the canopy layer, where interception is a function of available and maximum canopy storage capacity. Snowmelt is a simple degree-hour snowmelt algorithm that depends on a snowmelt factor:

$$M = mT, \quad \text{if } T > 0 \quad (4.5)$$

where M is rate of snowmelt (cm hr^{-1}), m is snowmelt factor ($\text{cm } ^\circ\text{C}^{-1} \text{ hr}^{-1}$) and T is average air temperature ($^\circ\text{C}$). Throughfall and snowmelt are the main input to unsaturated zone, but not all of the throughfall and snowmelt reaches the unsaturated zone. We assume a fixed percentage of the catchment area, namely the riparian area, to be saturated and therefore will produce saturation excess overland flow. Part of the snowmelt never reaches the unsaturated zone by becoming direct runoff and evaporation (sublimation). During winter months, the upper soil layer of some part of the catchment is known to freeze, creating an impermeable layer. We assume a fixed percentage of the snowmelt to be lost and manually calibrate this parameter.

Evapotranspiration is calculated using the relationship developed by *Thornthwaite and Mather* (1955) as a function of potential evapotranspiration, a vegetation coefficient (based on land use and vegetation), and average moisture content:

$$E = \begin{cases} 0, & \text{for : } \theta < \theta_w \\ c(t)E_P \left(\frac{\theta - \theta_w}{\theta_f - \theta_w} \right), & \text{for : } \theta < \theta_f \\ c(t)E_P, & \text{for : } \theta \geq \theta_f \end{cases} \quad (4.6)$$

where E_P is potential evapotranspiration (cm), $c(t)$ is a vegetation coefficient that varies throughout the year, θ is average soil moisture content ($\text{m}^3 \text{m}^{-3}$), θ_f is moisture content at field capacity ($\text{m}^3 \text{m}^{-3}$) and θ_w is moisture content at wilting point ($\text{m}^3 \text{m}^{-3}$). The actual evapotranspiration varies linearly between E_P , when soil moisture content is at or above field capacity, and becomes zero when soil moisture is below the wilting point. Monthly values of vegetation coefficients are based on *Jensen (1973)*.

Drainage is calculated using Darcy's law with the unit-gradient assumption. Using the *Campbell (1974)* parameterization yields:

$$N = K_s \left(\frac{\theta}{\phi} \right)^{2b+3} \quad (4.7)$$

where K_s is the saturated hydraulic conductivity, ϕ is soil porosity and b is a pore size distribution parameter. Since ϕ and b are generally correlated with K_s , we related these to K_s by linear regression with $\ln(K_s)$, fitted to the data provided by *Clapp and Hornberger (1978)*. This yields (*Teuling and Troch, 2005*):

$$\begin{aligned} \phi &= -0.0147 \ln(K_s) + 0.545 \\ b &= -1.24 \ln(K_s) + 15.3 \end{aligned} \quad (4.8)$$

Moisture above field capacity can drain to the underlying aquifer. Thus obtained drainage (recharge) is the input to the semi-distributed hsB model.

Runoff or direct runoff is mainly a fraction of throughfall, above a certain threshold, generated as saturation excess runoff in the riparian area. The riparian area is determined as a fraction of the whole catchment as derived from topographic analysis.

The parameters of the water balance model are listed in Table 4.1. Parameters related to partitioning of precipitation in rain and snow and canopy storage and evaporation parameters are based on *Boll et al. (1998)*. Interception is calculated for spruce trees based on *Lankreijer et al. (1999)*. The soil properties are based on field and laboratory measurements of soil samples.

Hillslope-storage Boussinesq (hsB) Model

The hsB model (*Troch et al., 2003b*) is a one-dimensional hydraulic groundwater model that describes the dynamics of saturated storage S along a hillslope. The hsB model is derived by combining the Boussinesq equation for sloping aquifers (using the Dupuit-Forchheimer assumptions) and the definition of storage capacity as

$$S_c(x) = D(x) w(x) f \quad (4.9)$$

Table 4.1: Parameters of the water balance model

Time step:	1.0	hr
Temperature threshold rain/ snow:	1.5	°C
Snowmelt factor (forest):	2.3	mm °C ⁻¹ day ⁻¹
Maximum canopy storage:	2.0	mm
Canopy evaporation during rain:	0.04	mm hr ⁻¹
Canopy evaporation factor during no rain (fraction of E_P):	0.5	
Residual moisture content:	0.02	
Moisture content at field capacity:	0.27	
Moisture content at wilting point:	0.11	
Saturated hydraulic conductivity:	1.00	mm day ⁻¹
Soil porosity:	0.45	
Fraction of riparian area:	0.02	
Soil depth (variable):	50.0	cm
Initial soil moisture storage:	8.0	cm

where $D(x)$ is average aquifer depth along the hillslope, $w(x)$ is hillslope width, and f is drainable porosity (or specific yield).

The resulting nonlinear hsB equation then reads

$$\frac{\partial S}{\partial t} = \frac{k \cos \alpha}{f^2} \frac{\partial}{\partial x} \left[\frac{S}{w} \left(\frac{\partial S}{\partial x} - \frac{S}{w} \frac{\partial w}{\partial x} \right) \right] + \frac{k \sin \alpha}{f} \frac{\partial S}{\partial x} + Nw \quad (4.10)$$

where k is saturated lateral hydraulic conductivity (to distinguish it from K_s used above), α is slope angle, and N is recharge rate (see *Troch et al.* (2003b) for more details).

The topographic parameters of hsB, hillslope length l , hillslope width function $w(x)$ and average hillslope gradient α are computed from a raster DEM. The 20 m resolution DEM of the Moxa catchment was broken up into individual hillslope elements (Figure 4.3). The field based perception of the channel network extent and a topographic analysis based channel network map was compared to determine the hillslope delineation.

4.2.3 Model input and conditions

The water balance model inputs consist of precipitation and temperature, which are collected at the observatory. Other forcings include potential evapotranspiration (estimated from weather data) and a vegetation coefficient. We calculated potential evapotranspiration by the ASCE Penman-Monteith (full) method using the REF-ET software developed at Kimberly, Idaho (*Allen*, 2000). Required site parameters are the elevation of the weather station above the ground surface, the elevation of the site above mean sea level, and the latitude of the site. Required data for hourly time-steps are mean hourly air

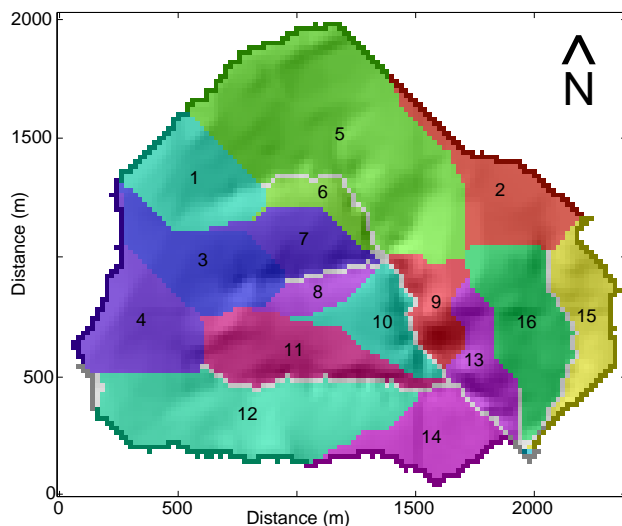


Figure 4.3: From catchment to hillslopes: hillslope delineation of Moxa catchment. The numbers and shades (colors) show different hillslopes.

temperature, relative humidity, wind speed, and solar radiation (estimated from illuminance data, see Section 3.3.2).

Actual evapotranspiration is based on moisture content, potential evapotranspiration, and a vegetation coefficient. The latter has a seasonal variation. It is assumed that the ET coefficient is 100% for the months November to March, 110% for the months April, May, September, and October, and 115% for the months June to August (*Jensen, 1973*).

The discharge data, used for model calibration and validation, are from occasionally sampled surface water levels at, and discharge through a V-Notch installed in the Silberleite (for detail see Section 3.3.2).

Simulation of the lumped water balance model was done at hourly time-steps, while hsB model simulation was performed at daily time-steps. Considering the size of the catchment and comparing the precipitation data collected from different rain gauges, spatially uniform input forcing was applied. For the same reason (small catchment) and for the reason of simulation time-steps (daily, larger than the time of concentration of the catchment), we did not consider discharge routing. For hsB model simulations, the initial water table conditions for different hillslopes were assumed to be the steady state water tables from estimated average recharge over a long period. We assumed fixed boundary conditions for the hsB model: no flow at the divide and zero water table head at the outlet.

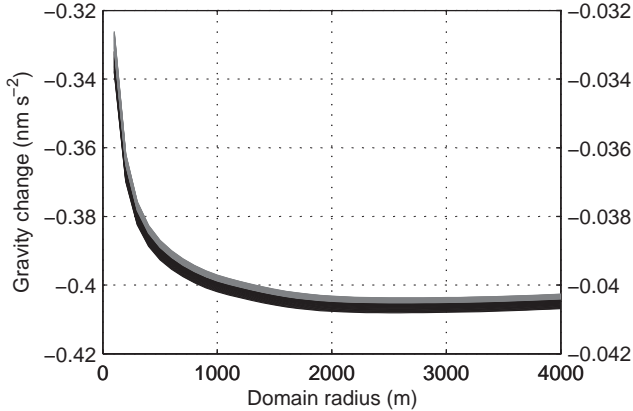


Figure 4.4: Range of change in gravity caused by 1 mm rise in soil moisture (black) or snow (gray) in 0.1 to 2.0 m soil or snow depth for different domain radius.

4.3 Sensitivity analysis of local gravity variation

Here we present the results of a sensitivity analysis testing the effects of storage change on gravity. The analysis is based on local topography and some simplifying assumptions of where and how much water storage changes in soils and aquifers. This analysis is done for both fast (near surface) and slow (aquifer) water storage changes as defined in Section 4.2. This analysis provides a better understanding of expected gravity residuals dynamics in our catchment.

For fast storage change, we consider a range of snow depth and soil layer thickness from 0.1 to 2.0 m with an interval of 0.1 m. In each case, a uniform distribution of unit (1 mm equivalent water) storage increase is assumed. This increase in storage is then converted to a change in density, the variation of which is caused by the assumed snow depth or soil layer thickness. Finally the change in gravity is calculated as described in Section 4.2.1. We also consider different horizontal domains around the gravimeter, by varying the radius from 100 to 4000 m with an interval of 100 m.

For slow storage change, we consider an aquifer parallel to the local topography, where the horizontal domain is limited to the catchment size. We vary the depth of the bedrock beneath the surface and calculate the change in gravity for a unit (1 mm) storage change in the aquifer. We further look at a condition where the aquifer is slowly filling up. We assume a situation, where a 10 m deep empty aquifer is gradually filled up and calculate the related gravity change.

We find $\sim 0.40 \text{ nm s}^{-2}$ instantaneous change in gravity caused by 1 mm change in soil moisture or equivalent snow storage. Most of the gravity variation due to fast storage change can be modeled if we consider a radius of about 1 km

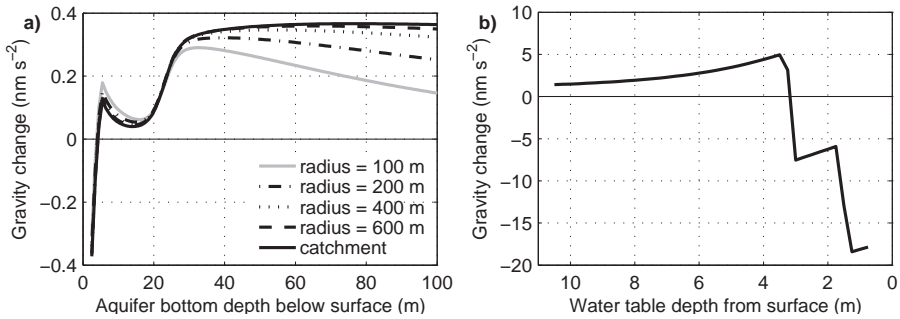


Figure 4.5: Analysis of slow storage change: a) Change in gravity caused by 1 mm rise in water table in a 2 m deep aquifer, when we move the aquifer vertically downward parallel to the topography. Lines show the effect on gravity for different domain radius and the catchment considered. b) Change in gravity caused by filling up of a 10 m deep aquifer, with the water table parallel to the surface topography.

around the gravimeter. We also find that the variation in snow depth or soil layer thickness has an insignificant effect on changing gravity (overlapping lines in Figure 4.4). This analysis confirms our previous findings (Chapter 2), where we used time series modeling to compute an impulse response function based on precipitation and gravity observation data. According to that black-box model, we found $\sim 0.35 \text{ nm s}^{-2}$ instantaneous change in gravity caused by 1 mm precipitation. The higher value in the current analysis can be explained by the fact that for a storage increase of 1 mm, a precipitation amount in excess of 1 mm is needed.

We find that the change in gravity varies both in sign and magnitude for the same amount of water storage change (Figure 4.5). Unlike near surface water storage, for saturated water storage (groundwater), the vertical extent of the domain changes because of temporal variation of the groundwater table. Thus, there are time varying relationships between the change in groundwater storage and gravity, because of topography and location of mass change. Figure 4.5 clearly shows a water table depth dependent temporal switch in the relationship between groundwater storage and gravity. Figure 4.5b shows different water table depths, where such a switching relationship can occur. We can justify the horizontal extent of saturated water storage component to be considered in gravity modeling, as we see gravity becomes less sensitive with increasing radius (overlapping lines in Figure 4.5a). We can also set a limit to the vertical extent of the hydrological domain, as below a depth of 30 m, gravity change becomes less sensitive to the depth of the aquifer (Figure 4.5a).

4.4 Gravity variation and hydrology

The sensitivity analysis (Section 4.3) is, however, limited to the assumption of a saturated water table and its temporal variation parallel to the topography. In a simple situation, where all considerable water storage changes are either above or below a gravimeter, gravity variation data can be useful in assimilation of storage changes. In reality, where considerable water storage changes occur both above and below a gravimeter, the question is if and how we can use the observed gravity field in hydrological modeling.

The following steps are considered here in applying and investigating gravity residuals in hydrological modeling:

1. From the available DEM, the gravity model is built as a distributed version of Equation 4.2 for density variations caused by different storage changes.
2. The parameters of the lumped water balance model are calibrated based on Nash-Sutcliffe model efficiencies (*Nash and Sutcliffe, 1970*) for fast (hourly) gravity variation.
3. The output from the lumped water balance model is then used as a forcing (recharge) for the semi-distributed hsB model.
4. The simulated saturated storage changes from hsB are used to calculate slow (daily) gravity variations.
5. Different simulations for different recharge conditions in hsB are tested, using Nash-Sutcliffe model efficiencies, to see how gravity field data can be useful in hydrological modeling.
6. The local hydrological effect on gravity is quantified and gravity variations with and without hydrological reductions are compared.
7. The final output of the hydrological models applied to the catchment is the discharge through the V-Notch near the gravimeter.

4.4.1 Fast storage change

The lumped water balance model gave us an estimate of hourly variation in average soil moisture and snow storage for the area around the gravimeter. These storage changes are redistributed spatially with the aid of topographic information and Equation 4.2 is applied to compute gravity variations. Fast gravity variation, modeled from soil moisture and snow storage change, is compared with observed gravity variation (Figure 4.6). Effective soil depth (soil depth \times porosity) for the lumped model was calibrated using hourly gravity data and Nash-Sutcliffe model efficiencies as the measure for goodness of fit (Table 4.2). The model results agree well with the observed gravity signal both in magnitude and dynamics. For a given soil depth, porosity does not play a significant role in changing the fluxes, as the average soil column never

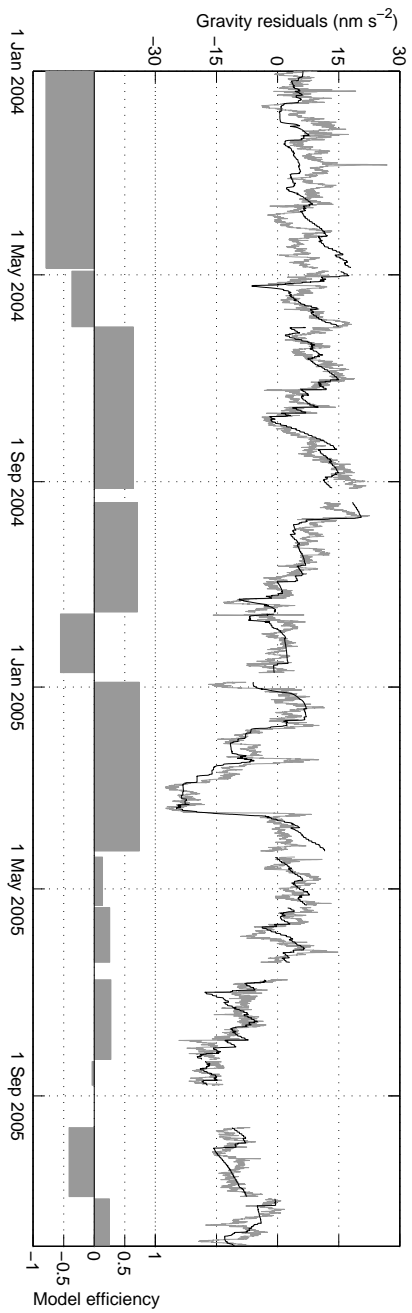


Figure 4.6: Observed (gray) and modeled (black) fast gravity variation. The modeled residuals contain effects of changes in soil moisture and snow storage. The gray bars at the bottom show the model efficiency (Nash-Sutcliffe coefficients) for different periods separated by missing data.

Table 4.2: Parameters for lumped water balance model (Nash-Sutcliffe model efficiencies are calculated for gravity residuals)

Soil depth (cm)	20.0	30.0	40.0	50.0	60.0	70.0	80.0
Efficiency	0.57	0.65	0.68	0.70	0.67	0.60	0.56
Field capacity (%)		20.0	25.0	27.0	30.0	40.0	
Efficiency		0.64	0.66	0.70	0.65	0.60	

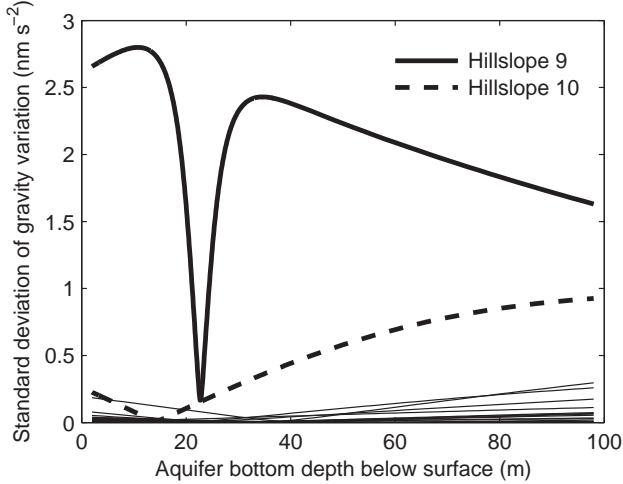


Figure 4.7: Effect of different hillslopes in the catchment on gravity variation due to saturated water storage change. Hillslope numbers are shown in Figure 4.3. Legend shows only the most effective hillslopes, while the other hillslopes' effects are plotted using thin gray lines.

reaches saturation. However, as we used field capacity in affecting actual evapotranspiration and drainage, we looked at the effect of varying field capacity (Table 4.2).

Table 4.2 compares the efficiency of the lumped water balance model in reproducing the gravity residuals. We find generally good agreement between observed and modeled gravity residuals. The poor model efficiency during some periods indicates other effective dynamics (e.g. lateral redistribution of saturated water content) not considered in modeling of the fast storage change. In the modeled gravity, as presented in Figure 4.6, negative spikes can be explained by quick addition to water storage (e.g. rain, snow), while positive spikes can be explained by snowmelt.

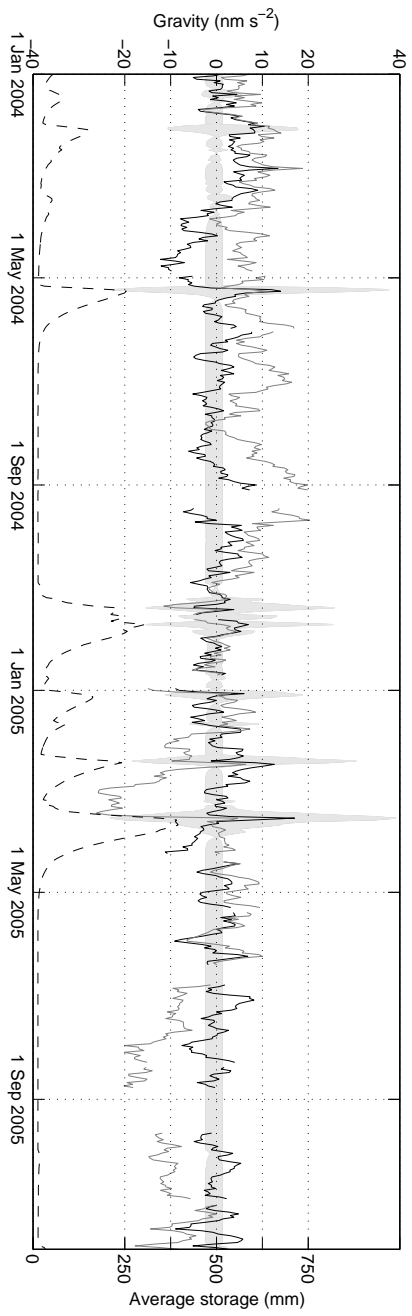


Figure 4.8: Range of gravity variation for a varying bedrock depth, ranging from 2 to 100 m below surface (shaded gray area), gravity residuals before (solid black line) and after (solid black line) local hydrological reductions, along with modeled catchment average saturated water storage condition (dashed black line).

Table 4.3: Parameters for semi-distributed hsB model (Nash-Sutcliffe model efficiencies are calculated for discharge)

Drainable porosity (%)	0.05	0.10	0.15	0.20	0.25
Efficiency	0.55	0.60	0.59	0.57	0.56
Hydraulic conductivity (m hr ⁻¹)	0.80	0.90	1.00	1.10	1.20
Efficiency	0.59	0.60	0.60	0.60	0.59

4.4.2 Slow storage change

The hsB model, coupled with the water balance model, provides estimates of daily variation in saturated water storage for different hillslopes in the catchment. Ranges of slow gravity variations were calculated from saturated water storage change for all the hillslopes of the catchment with changing bedrock positions (2 to 100 m below surface). Analyzing the gravity variation caused by saturated storage changes from individual hillslopes, we find that hillslope 9 and 10 (see Figure 4.3 for their location within the catchment) contribute most strongly to gravity changes. Figure 4.7 shows the effect of all hillslopes in changing gravity by saturated storage dynamics. The switch in relationship between gravity and saturated storage is clearly visible. The change in this relationship occurs at a different depth for different hillslopes, which can be explained by the different positions of the hillslopes, relative to the gravimeter. Considering the complexity in the groundwater–gravity relation, we decide to employ gravity variations to calibrate the depth to the bedrock of hillslopes 9 and 10. However, we do not neglect the effect of saturated water dynamics on gravity and look at the likely range of gravity variations modeled from saturated water dynamics. In Figure 4.8, the modeled slow gravity variation range is compared with the residuals obtained from observed and modeled gravity variation.

The parameters of the hsB model (effective drainable porosity and hydraulic conductivity) were calibrated based on Nash-Sutcliffe model efficiencies for observed and modeled discharge (Table 4.3) through the V-Notch. Figure 4.8 clearly demonstrates that peaks in saturated water storage can be associated to some positive peaks in temporal gravity variation. However, we also encounter periods of low storage conditions or no storage changes, with observed gravity variations. Hence, this model does not ensure capturing gravity variation during low storage conditions. During these conditions, local storage change may occur in the form of redistribution, which may not change the global storage quantity. The obvious explanation for not capturing gravity variations during low storage conditions is the lack of detailed information (e.g. location) regarding groundwater redistribution. Another possible explanation is that the observed gravity variations during low storage conditions are not caused by local hydrological changes.

4.4.3 Hydrological gravity reductions

Using the results presented in Figure 4.8, we optimized the effect of saturated water storage change on gravity variation for hillslope 9 and 10. The effective bedrock positions of hillslope 9 and 10 are ~ 22.5 and 12.5 m below the surface, respectively. The local hydrological effects on gravity are calculated using the results obtained from the sensitivity analysis and hydrological model simulations. Observed gravity residuals are reduced for the local hydrological effect, and the resulting gravity residuals are presented in Figure 4.8. The hydrological models explain 80% of the variance of the observed gravity residuals, which is $65.42 \text{ nm}^2 \text{ s}^{-4}$, while the variance of gravity residuals reduced for local hydrological effect is $12.85 \text{ nm}^2 \text{ s}^{-4}$.

4.4.4 Final model output

We examine the final model output by comparing modeled with observed discharge at the V-Notch. For various recharge conditions (i.e. lumped model output), we performed different simulations of the hsB model and checked the model performance, quantified as Nash-Sutcliffe model efficiencies with respect to discharge (Table 4.2). We also examined the hsB model parameters and found the hydraulic conductivity to be less effective than the drainable porosity (shown in Table 4.3).

Figure 4.9 shows a comparison of observed and modeled discharge through the V-Notch near the gravimeter. The model results agree well with the observed signal both in magnitude and dynamics during some periods, while during other periods the model over-estimates the discharge. While comparing the hydrographs, please note that during some winters, the data collection system was hampered by frozen surface conditions. As a result, some snowmelt events are missing in the observed discharge data.

4.5 Discussion

We employed terrestrial gravity observations from a single location to constrain hydrological models in a small catchment. A simple lumped water balance model, constrained by fast gravity variations, gives us robust and effective input conditions for the semi-distributed hillslope-storage Boussinesq model. The hsB model successfully reproduces the discharge magnitude and dynamics. Despite the fact that the parameters used in the lumped water balance model are averaged over the entire catchment, our models give encouraging results for both hydrology and gravity. Considering the observed gravity change as an additional integrator of catchment-scale hydrological response, and therefore using it to constrain hydrologic models for that catchment, proves to bring a new way of validating water balance estimates.

Geographical position relative to the gravimeter plays an important role in the relationship between storage and gravity variation. The topography based analysis, using available DEM and possible storage variations distributed in the

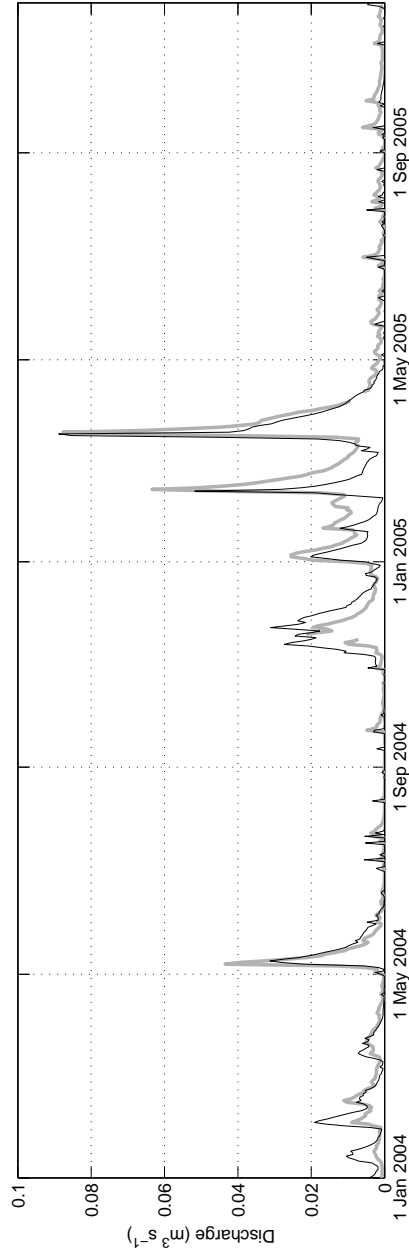


Figure 4.9: Observed (gray) and modeled (black) discharge through the existing V-Notch near the gravimeter. Note that there are missing data in observed time series.

catchment, shows the extent of the hydrological domain affecting point-scale gravity. Despite the encouraging results we obtained in hydrological modeling, this chapter also shows the limitations in modeling of temporal gravity variation caused by hydrological redistribution in the local geophysical conditions, where storage changes occur both above and below a gravimeter. However, by providing the likely range of variation in gravity caused by local hydrological changes, we made it possible to produce a gravity time series, free from local hydrological effects.

Hinderer et al. (2006) investigated seasonal changes of the earth's gravity field from GRACE (Gravity Recovery and Climate Experiment (*Tapley et al.*, 2004a)), and made a comparison with surface gravity measurements in Europe from the GGP network and hydrological models for continental soil moisture and snow. Following their findings and discussions, terrestrial gravity variations observed at the point-scale have to be free from local effects, in order to apply in larger-scale hydrological investigations. In this study, we provided calculations of gravity variations caused by local hydrological changes that explain 80% of the observed gravity variations.

Considering the complex geophysical conditions and limited knowledge of sub-surface variability in detecting local hydrological effects, satellite geodesy has the potential of simplifying the geophysical conditions to some extent. Once local gravity variations are free from local effects, GRACE and GRACE-like projects can be used in combination with superconducting gravimeter data for basin-scale hydrological modeling and validation.

Potential of satellite gravity measurements in hydrological modeling

5.1 Introduction

Since its launch in March 2002, the Gravity Recovery and Climate Experiment (GRACE) (*Tapley et al.*, 2004b) mission has been providing estimates of surface mass anomalies for the entire globe. Despite the coarse spatial (a few hundred kilometers) and temporal (1 month) resolution of GRACE estimates, the mission has proven to deliver valuable data for continental scale river basin water balance studies. The success of the GRACE mission in estimating terrestrial water storage (TWS) changes has been demonstrated in many studies (e.g., *Tapley et al.* (2004a); *Wahr et al.* (2004); *Ramillien et al.* (2005); *Syed et al.* (2005); *Swenson and Milly* (2006)). Direct comparison of terrestrial water storage (TWS) estimates from GRACE with in-situ hydrological observations also shows good agreement (*Swenson et al.*, 2006). Using GRACE and other observations, regional evapotranspiration (e.g., *Rodell et al.* (2004); *Ramillien et al.* (2006); *Boronina and Ramillien* (2008)) and snow mass (e.g., *Niu et al.* (2007)) have been estimated successfully. All these studies (*Güntner* (2008) reported a detailed overview), mostly conducted in large river basins (e.g., Amazon, Mississippi, Ganges, Zambezi), recommended application of GRACE data in constraining hydrological models. On the contrary, very few studies (e.g., *Niu and Yang* (2006); *Ngô-Duc et al.* (2007); *Zaitchik et al.* (2008); *Werth et al.* (2009)), applied GRACE data to improve land surface models (LSM).

As the temporal and spatial variation of the TWS inferred from GRACE is an integrated signal, the challenges remain in quantifying spatio-temporal relationships with the different storage and flux components in the hydrological cycle. To realize the full potential of GRACE for hydrology and water man-

agement, the derived regional scale, column-integrated, monthly water storage anomalies must be disaggregated horizontally, vertically and in time (*Zaitchik et al.*, 2008). Recently released GRACE gravity field coefficients (release 04, RL04) represent a significant improvement over previous releases and allow mapping more accurate mass anomalies with higher spatial resolution. Based on all released gravity field coefficients, different research centers calculate surface mass anomalies (estimates of TWS change) for different spatial resolutions and make them available on the web.

In this chapter we focus on the value of such GRACE data in a smaller, partly mountainous, partly semi-arid basin, namely the Colorado River Basin (CRB). We investigate TWS change estimates from different releases at different resolutions, in combination with hydrologic modeling and in-situ data to assess the potential of GRACE data in mountainous and semi-arid regions.

5.2 Materials and methods

The Colorado River is among the most heavily regulated river basins in the world, providing water supply, irrigation, flood control, and hydropower to a large area of the Southwestern United States. The basin (Figure 5.1) covers about 637,000 km² and spreads over the southwestern US and a small portion of Mexico. Almost 90% of the river's annual streamflow originates from the snowpack in the Rocky Mountains (Upper CRB), while the desert-like part (Lower CRB) receives most of its water from ephemeral tributaries and seasonal rain (summer monsoon precipitation). The man-made surface storage capacity of the basin consists of almost 74 km³ in over 90 reservoirs. See *Christensen et al.* (2004) and *Troch et al.* (2007) for more information on the Colorado River Basin.

5.2.1 The Gravity Recovery and Climate Experiment

The GRACE project Science Data System (SDS) delivers monthly models of the earth's gravity field. The SDS centers are the Center for Space Research (CSR, USA), GeoForschungsZentrum (GFZ, Germany) and Jet Propulsion Laboratory (JPL, USA). CSR, GFZ, and JPL all use different algorithms to compute gravity field coefficients from the raw GRACE observations, although they have agreed to use many similar background models. GRACE data are available since April 2002. The most recent dataset, based on the latest processing standards (RL04), is provided as an operational product in the form of global gravity fields. In producing these fields, several known gravity effects, such as tides of the solid earth, the oceans and the atmosphere, and non-tidal oceanic and atmospheric mass variations, have been taken into account. Thus, theoretically, mainly the hydrological signal due to water mass variations on the continental area including mass variations of ice caps and glaciers, can be expected to remain in the time-variable gravity fields. As required for hydrological applications, the global gravity fields, represented by sets of spherical harmonic

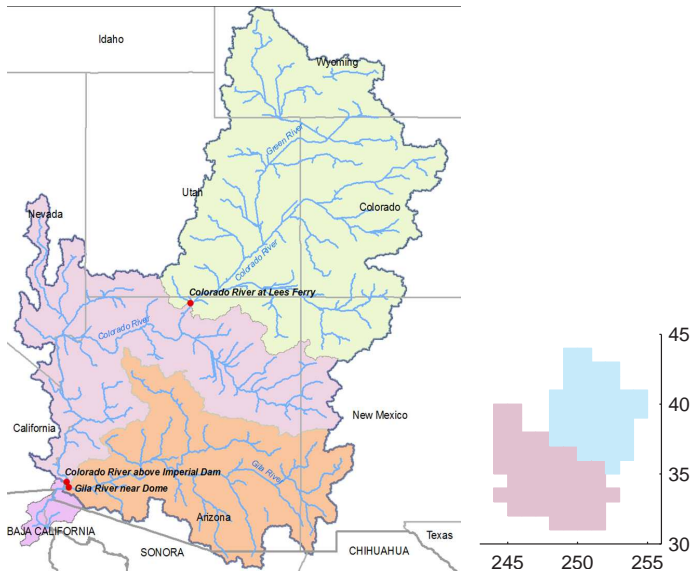
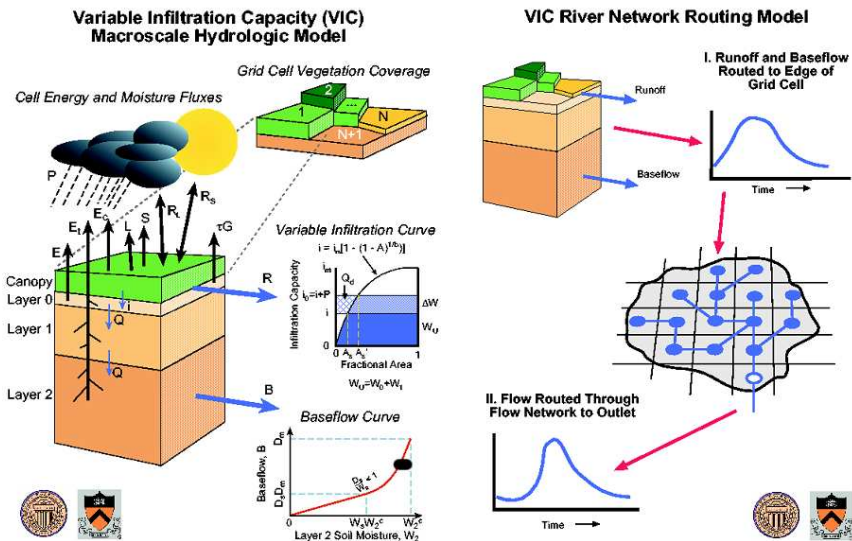


Figure 5.1: The Colorado River basin. Inset: Upper and Lower Colorado delineation at 1 degree resolution.

coefficients, can be transferred into mass anomalies at the earth’s surface with units of mm water equivalent (see Section 1.3).

For this study we used release 04 (RL04) of the monthly gravity field product distributed by the SDS centers. The RL04 coefficients represent a significant improvement over previous releases of the data. The most significant differences are the use of a new mean gravity field model determined using more GRACE data, the inclusion of an ocean pole tide as a background model, and the use of a new ocean tide model extended to higher resolution. In addition, all centers modified their computation strategy in order to better estimate the degree 2 zonal term Stokes coefficient, $C_{2,0}$ (Chambers, 2006). For more information, see the processing standards documents, available on the data archive site (<ftp://podaac.jpl.nasa.gov/grace/doc>).

Based on CSR RL04, GFZ RL04 and JPL RL04 gravity field coefficients, surface mass anomalies were calculated at different research centers and made available on the web. GRACE estimates of surface mass anomalies spatially averaged over the CRB and monthly mass grids with a spatial interval of 1 degree are obtained from the GRACE Tellus website (<http://grace.jpl.nasa.gov/data/>). It must be noted that GRACE does not actually resolve spatial details of 1 degree and at this moment the effective resolution is 4 to 5 degrees (solutions up to degree and order 40). A map of surface mass anomalies computed from raw GRACE data will be dominated by errors in the short wavelength (high degree) Stokes coefficients. Using additional data and models (e.g., smoothing), the GRACE gravity fields are corrected for different errors, resulting in a new set of gravity coefficient anomalies for each month (Swenson *et al.*, 2008). For



Source: <http://www.hydro.washington.edu/Lettenmaier/Models/VIC/VIChome.html>

Figure 5.2: Schematic representation of the Variable Infiltration Capacity (VIC) model and the VIC river network routing model.

detailed information regarding the conversion of release 04 gravity coefficients into maps of equivalent water thickness, see *Chambers* (2006).

5.2.2 Hydrological modeling

The Variable Infiltration Capacity model (VIC; Figure 5.2; *Liang et al. (1994)*) is a macro-scale hydrologic model that solves the full water and energy balances at a user-specified spatial resolution (here 1/4 degree), incorporating meteorological forcing data as input (precipitation rate, air temperature, vapor pressure, air pressure, downward shortwave radiation, downward longwave radiation and wind speed). For the continental US such a dataset was compiled from observations by *Maurer et al. (2002)* at a temporal resolution of 3 hours. This dataset has recently been expanded by the University of Washington to include data up to 2005. Our VIC model was calibrated to monthly naturalized flows (*Prairie and Callejo, 2005*) at Lees Ferry and Imperial Dam, with efficiencies of 0.88 and 0.85, respectively. VIC storage changes are calculated at sub-daily timescales; we aggregate these changes to monthly timescales to allow for direct comparison with the GRACE estimates.

The main water storage components modeled by VIC are soil moisture in 3

layers and snow water equivalent (SWE). The saturated and unsaturated zone are not explicitly resolved. However, based on the fact that baseflow occurs from the lowest soil layer, the upper 2 layers are considered here as the unsaturated storage, while the lowest layer is considered as the saturated storage. The whole basin was divided into the Upper and Lower CRB (Figure 5.1) to perform the analysis.

5.2.3 In-situ data sets

In-situ data regarding the space-time variability of the hydrologic stores (snow, reservoir storage and groundwater) and fluxes (precipitation and stream flow) were collected from different sources. Monthly precipitation data were obtained from 392 stations of NCDC–NOAA, of which 163 and 227 stations are in the Upper and Lower CRB, respectively. Daily snow water equivalent data were collected from SnoTel–NRSC for 154 stations (122 and 26 stations for the Upper and Lower CRB). Precipitation and snow data are evenly distributed, covering most of the basin. Furthermore, we obtained groundwater, stream flow and reservoir storage data from NWIS–USGS for a handful of stations. After quality control of those data, we could use 38 groundwater stations (8 and 30 stations for the Upper and Lower CRB).

As GRACE data represent monthly mass anomalies, the comparison with different datasets (modeled and observed) requires the computation of storage anomalies. For all data, the averages for the time period between 2003 and 2005 were subtracted in order to allow comparison with GRACE anomalies. The available data have different spatial and temporal resolutions. Comparison of in-situ data with GRACE estimates was not possible for all the variables, because of limited data availability.

5.3 Analysis and results

5.3.1 Basin average GRACE and VIC

The surface mass anomalies computed from different GRACE products show appreciable variation (Figure 5.3). As expected, the amplitudes dampen and the correlation between the solutions increases with an increasing radius of smoothing. We still find that CSR and JPL data are converging at 500 km smoothing (correlation coefficient of 0.87), while GFZ data are clearly different. See Table 5.1 for the detailed correlation structures. We further investigate the (mass) storage variations, estimated from GRACE data and modeled by VIC (Figure 5.4).

Both basin average and the average of 1 degree distributed GRACE estimates of total storage anomalies are generally in good agreement with VIC simulated storage anomalies (Figure 5.4). All three solutions more or less behave in a similar way. With regard to comparison with VIC simulation results, the average of distributed GRACE data performs better than the basin average GRACE estimates (See Table 5.1 for the results). This stimulated us

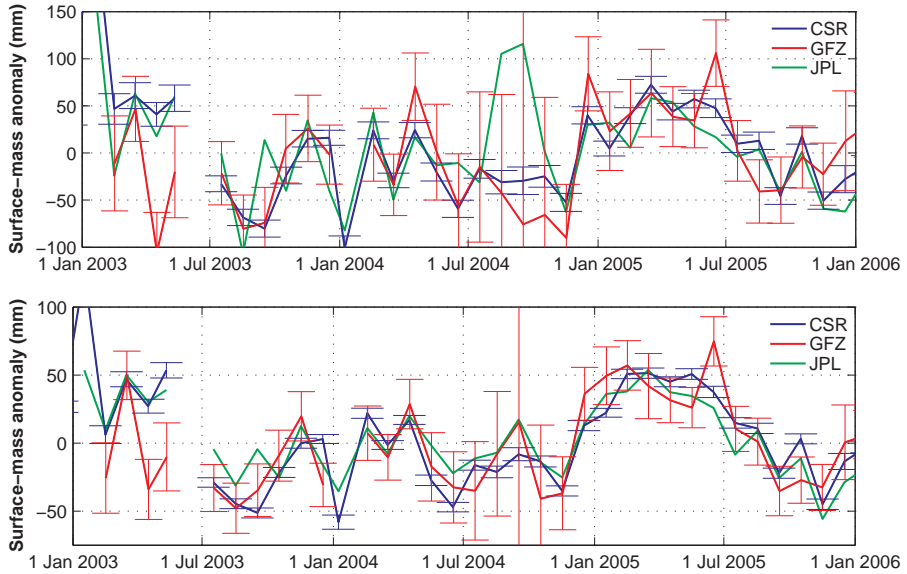


Figure 5.3: Basin average surface mass anomaly (mm) from different SDS centers, with different smoothing radius: Top – 300 km and bottom – 500 km. Uncertainty due to errors in the GRACE data is based on the method described in *Wahr et al. (2004)*.

Table 5.1: Correlation between VIC simulated basin-average storage anomaly and two GRACE estimates

	VIC	CSR-A	CSR-B
VIC	1	0.88	0.57
Average of distributed GRACE (CSR-A)	0.88	1	0.77
Basin average (CSR-B)	0.57	0.77	1
	VIC	GFZ-A	GFZ-B
VIC	1	0.77	0.70
Average of distributed GRACE (GFZ-A)	0.77	1	0.82
Basin average (GFZ-B)	0.70	0.82	1
	VIC	JPL-A	JPL-B
VIC	1	0.72	0.60
Average of distributed GRACE (JPL-A)	0.72	1	0.83
Basin average (JPL-B)	0.60	0.83	1

(See Figure 5.4 for related plots)

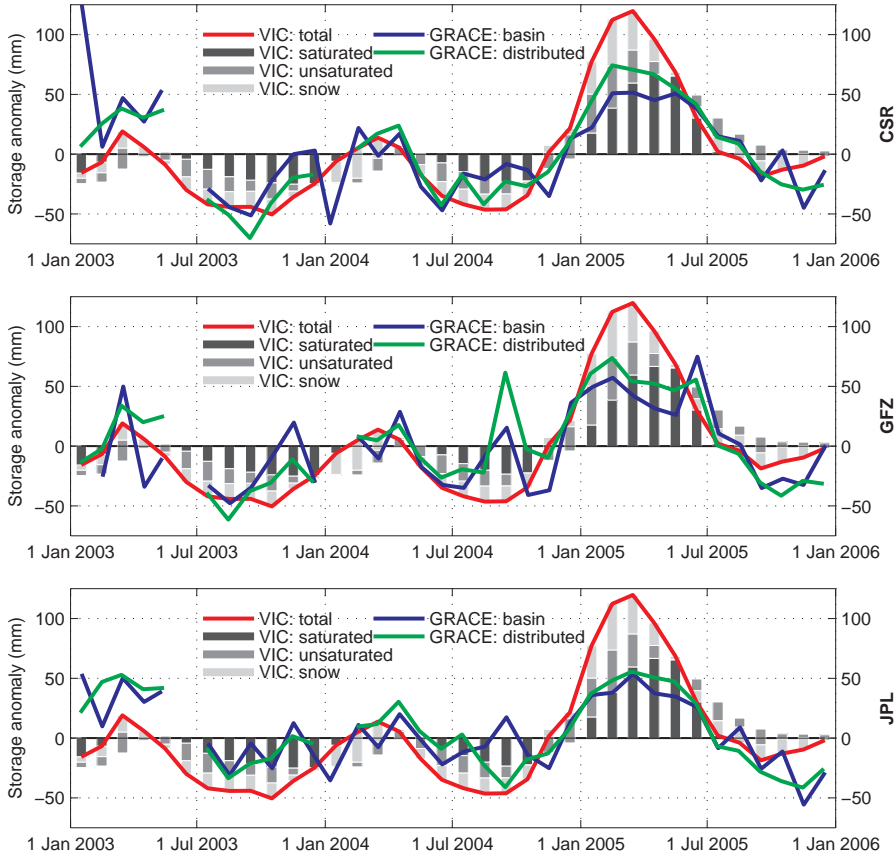


Figure 5.4: VIC simulated basin-average storage anomaly along with its distribution and two GRACE estimates, from three different SDS centers (labeled at right). Stacked bars show anomalies for different storage components modeled in VIC.

to compare the distributed GRACE data with VIC simulations. Any of the distributed dataset could be selected for the distributed analysis. However, we selected CSR solutions for the investigation of distributed GRACE data, as it shows better correlations with VIC than the others (Table 5.1).

Although the monthly storage dynamics of GRACE and VIC match well, VIC's seasonal cycle shows a larger amplitude compared to that of GRACE. It is important to note that the VIC version we employed, simulates naturalized flow rather than observed or controlled flow (e.g. by dams). As a result, VIC does not necessarily provide actual storage conditions. On the other hand, GRACE is affected by present storage conditions that can be observed from in-situ data, provided there are enough data points/ values to estimate the spatio-temporal variability. Another important factor to realize is that GRACE data at the basin boundary will be influenced by the surroundings outside the basin, which are not considered in the calculation of VIC simulated storage change.

5.3.2 Distributed GRACE

It has already been mentioned that GRACE does not actually resolve at 1 degree spatial variations. For any application of GRACE data, the effective resolution is 4 to 5 degrees. Solutions up to degree and order 40 were considered in estimating distributed surface mass anomalies in *Chambers* (2006) (data used in this study). However, we can study the patterns of 1 degree distributed GRACE data, with the understanding that the signal in a single cell is influenced by the surrounding cells. Figures 5.5 and 5.6 show spatial patterns observed by GRACE in our basin. The effects of smoothing radius are clearly visible both in the amplitude (Figure 5.5) and variability (Figure 5.6). Figures 5.5 and 5.6 also show the clear differences between the different GRACE products.

The GRACE data smoothed at 500 km radius can be considered more realistic, as that comes closer to the spatial resolution GRACE can actually resolve. Looking at the average storage anomalies (bottom panel of Figure 5.5), we see the basin is divided into 2 parts, namely, North-Western and South-Eastern parts. In terms of variability, the division is closer to the Upper and Lower (bottom panel of Figure 5.6) basins. This can be explained by the physical and hydrological characteristics of the basin. It is the Upper CRB that receives more water from snowfall and most of the basin's streamflow is derived from this source.

In Figure 5.7 we show different water storage components modeled by VIC and GRACE estimates for Upper and Lower Colorado basin. The relations found are summarized in Table 5.2. This analysis demonstrates that the part of the basin with more variability can be easily recognized by GRACE, as was shown in numerous GRACE related studies in large river basins (described in Section 5.1).

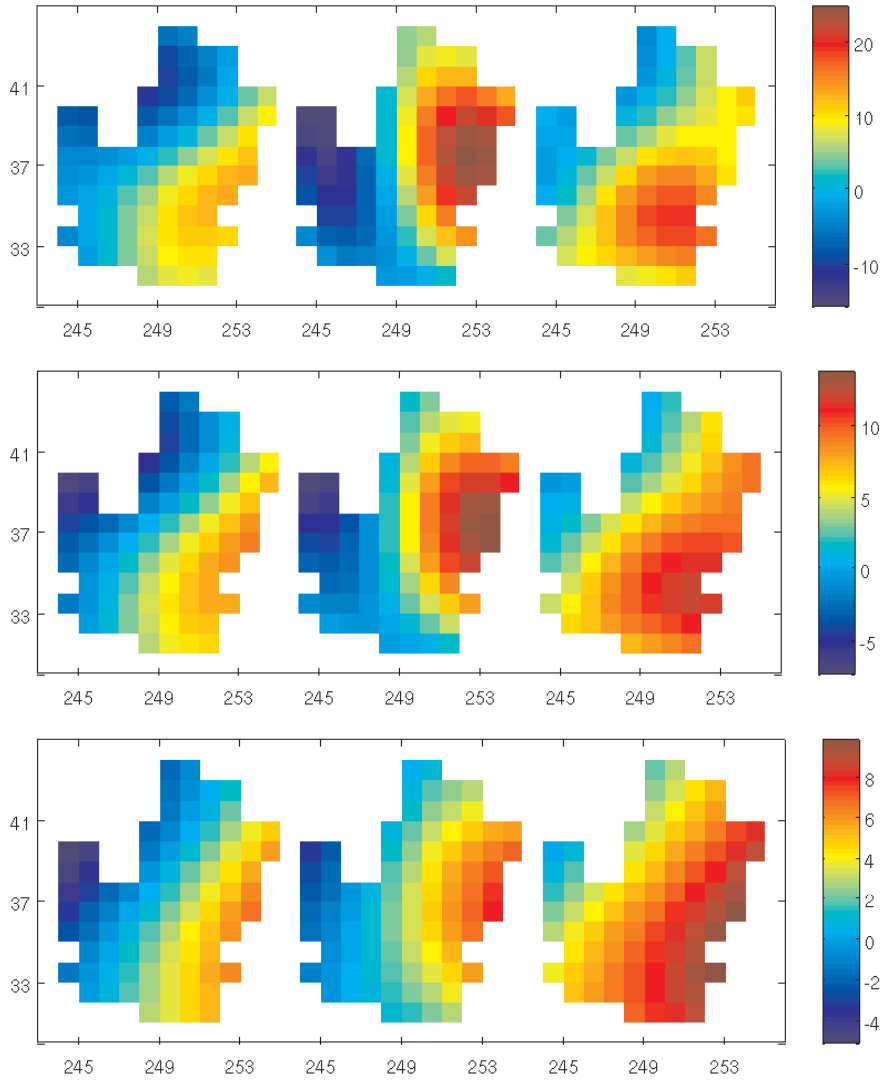


Figure 5.5: Maps of mean surface mass anomaly (mm) from distributed GRACE estimates: CSR, GFZ and JPL from left to right, with different smoothing radius: Top – 0 km, middle – 300 km and bottom – 500 km. Scales are in mm water thickness.

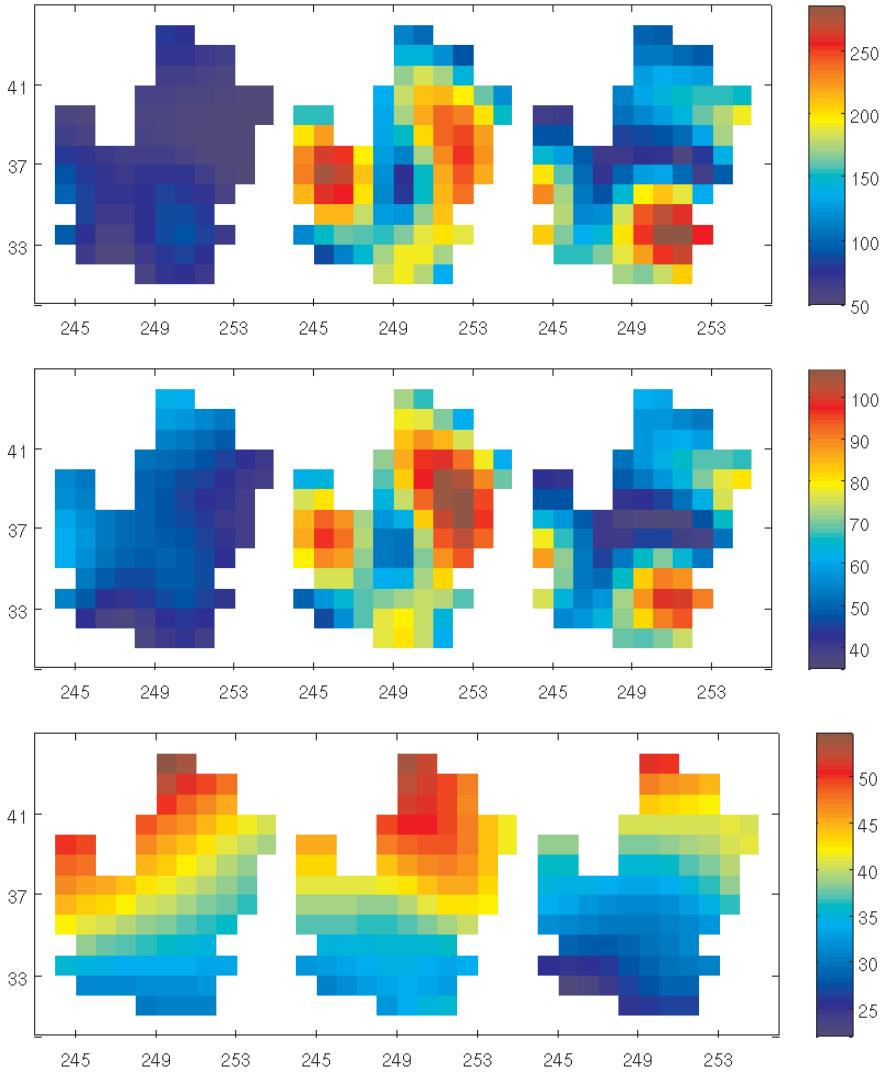


Figure 5.6: Maps of variation in surface mass anomaly (standard deviation in mm) from distributed GRACE estimates: CSR, GFZ and JPL from left to right, with different smoothing radius: Top – 0 km, middle – 300 km and bottom – 500 km. Scales are in mm water thickness.

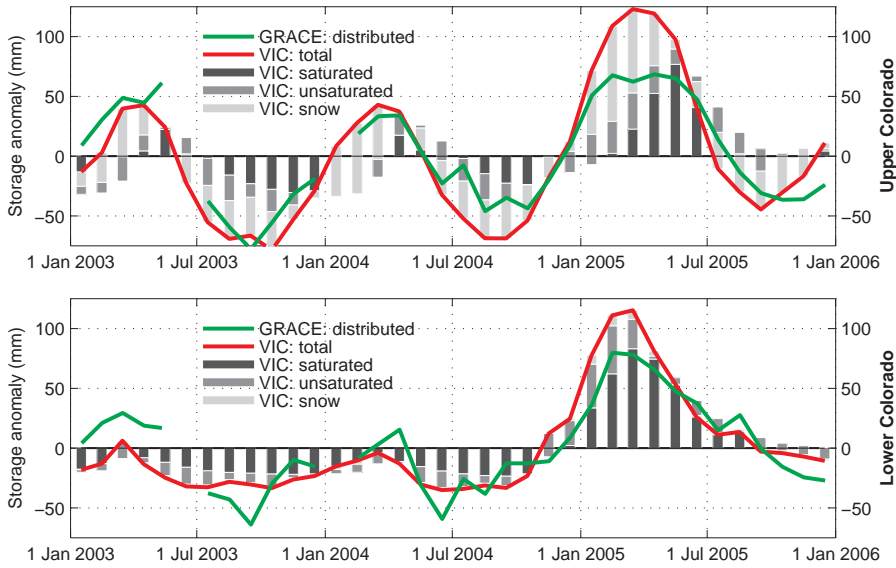


Figure 5.7: VIC simulated storage anomaly for the Upper (top) and Lower (bottom) CRB along with its distribution and average of distributed GRACE estimates (CSR-500 km smoothing). Stacked bars show anomalies for different storage components.

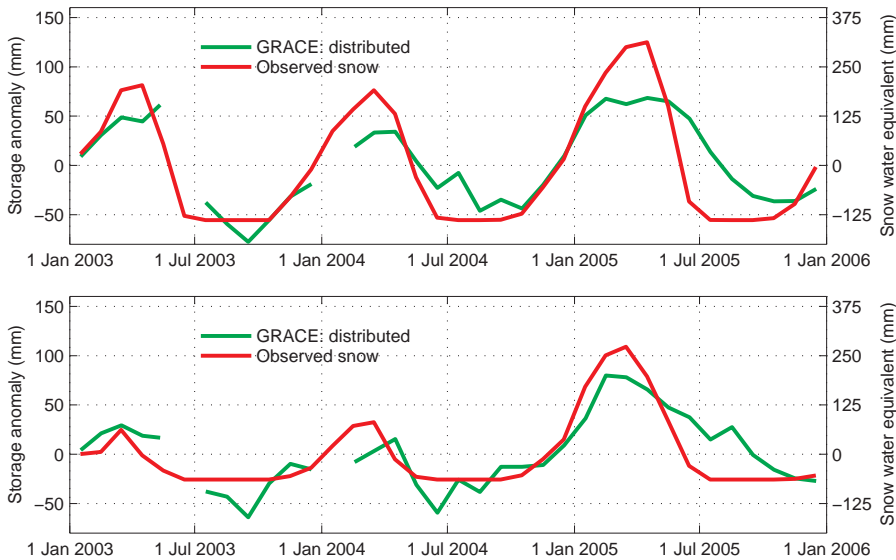


Figure 5.8: Observed anomaly in snow data for the Upper (top) and Lower (bottom) CRB and average of distributed GRACE estimates (CSR-500 km smoothing).

Table 5.2: Correlation between different variables obtained from GRACE, VIC and in-situ data

Correlation between variables	Upper Coloraro	Lower Coloraro	Total Coloraro
Basin average GRACE:			
CSR and GFZ (smoothing 300 km)			0.66
GFZ and JPL (smoothing 300 km)			0.70
JPL and CSR (smoothing 300 km)			0.25
CSR and GFZ (smoothing 500 km)			0.74
GFZ and JPL (smoothing 500 km)			0.73
JPL and CSR (smoothing 500 km)			0.87
VIC total storage with GRACE	0.92	0.86	0.90
VIC snow storage with GRACE	0.77	0.71	0.76
VIC soil moisture with GRACE	0.74	0.60	0.69
VIC ground water with GRACE	0.50	0.81	0.69
Observed snow with GRACE	0.85	0.79	0.84
Observed groundwater with GRACE	0.19	0.55	0.63
Observed rainfall with GRACE	-0.04	0.29	0.18

5.3.3 Distributed GRACE and observed data

Finally we look at the GRACE estimates (CSR–500 km smoothing, as that showed the best agreement) of storage anomaly and observed snow water equivalent data. Snow data was selected because of adequate data availability and validity of relatively simple averaging without many extra parameters. For example, for converting groundwater data to storage we need to know aquifer parameters. As expected, we find more snow storage variation and agreement with GRACE in the Upper CRB (Figure 5.8). It is interesting to note that GRACE appears to lag behind the in-situ snow data. As reported in Table 5.2, we have performed comparison with other available data (groundwater, rainfall), but no significant correlation was found. However, observed groundwater data are better correlated with distributed GRACE in the Lower CRB.

5.3.4 Potential of GRACE data

The distributed storage estimates from GRACE data show enough evidence of good correspondence with the basin average estimates from GRACE. Furthermore, some spatial patterns are visible in the distributed GRACE data. We finally investigate spatially distributed temporal correspondence between VIC and GRACE (Figure 5.9). We use two sets of VIC simulation results: First

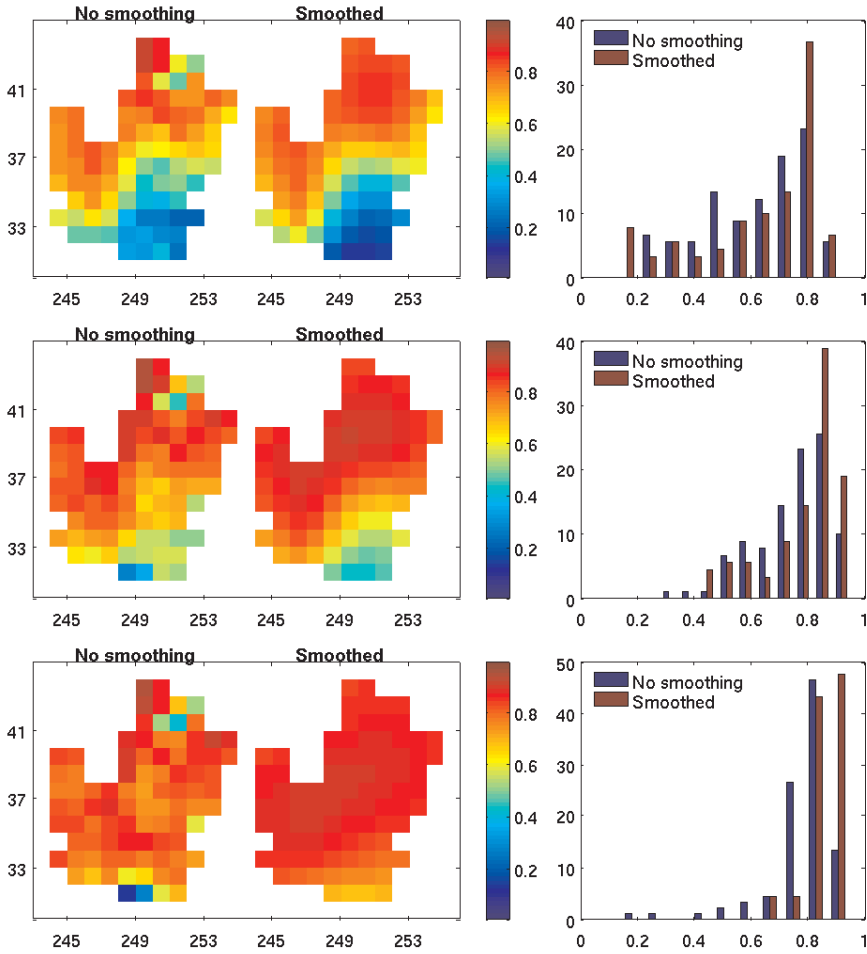


Figure 5.9: Left panels: Spatially distributed temporal correlation between GRACE and VIC. The smoothing radius for distributed GRACE are: Top – 0 km, middle – 300 km and bottom – 0 500 km. The headers show if VIC data were smoothed or not. Right panels: Histograms of correlation coefficients shown as percentage of basin area.

the results as were simulated and second the results smoothed with a radius of 500 km (similar to GRACE).

By smoothing VIC simulation results, we get a better correlation with GRACE, but at the same time the spatial variability is lost. Moreover we did not use any hydrological data or model outside the CRB. As a result, storage information near the boundary is lost by leakage, while no outside information is there to compensate for the loss.

5.4 Discussion

The success of macroscale hydrological models depends on how accurately spatially variable model parameters and input forcings represent the true basin conditions. The reported agreement found between GRACE and VIC storage dynamics provides some confirmation that our VIC model is appropriate for modeling the hydrology of the CRB, and that the meteorological forcing can be considered adequate. However, the limited agreement regarding the amplitude may raise questions about the calibrated model parameters, as well as applicability of GRACE in the CRB, given its size and water storage variability. Although the model performance in terms of simulated discharge was found to be good, the storage distribution and dynamics do not have to reflect the true conditions. In order to apply GRACE data in a basin like the CRB, we at least need to combine hydrological information from the surrounding basins. That will require a combination of multiple hydrological models. The differences in various GRACE products for the same basin also need to be addressed.

The objective of this thesis was to investigate the possibility to detect variations in terrestrial water storage from ground-based and satellite observations of the earth's gravity field. This chapter provides a summary of the main results and conclusions of this investigation (Section 6.1), puts these results into perspective (Section 6.2), and presents an outlook for future research on this topic (Section 6.3).

6.1 Conclusions

6.1.1 Terrestrial gravity

By time series analysis (Chapter 2) and distributed hydrological modeling (Chapter 3) techniques we detected and quantified the hydrological component of terrestrial gravity variation, as observed by a superconducting gravimeter at the Geodynamics Observatory Moxa, Germany. Both approaches yielded encouraging results, and served complementary objectives. Time series modeling provided us with a simple yet effective technique to correct for precipitation effects on short-term gravity residuals. Analysis of deep groundwater and gravity residuals demonstrated different dynamics present in the catchment. Distributed water balance modeling explained both short and long-term behavior of the gravity signal. The hydrological model (Chapter 3) also confirmed the findings from our time series analysis (Chapter 2).

We continued by applying terrestrial gravity observations to aid catchment-scale hydrological modeling (Chapter 4). In that application, we used simple water balance models to simulate catchment water storage dynamics and the related variation of gravity at a point in the catchment. We classified the water

storage changes into fast and slow changes to analyze the hydrological effect on gravity and to evaluate hydrological models by means of gravity variation. The fast storage changes are the changes in root zone and snow water content, calculated at hourly time steps. The slow storage changes are the changes in saturated water content, calculated at daily time steps.

By means of a sensitivity analysis, we showed what parts of the gravity variation could be estimated from hydrological models. We found that a 1 mm change in soil moisture or snow water equivalent causes $\sim 0.40 \text{ nm s}^{-2}$ instantaneous change in gravity. We also showed that the horizontal extent of the hydrological domain affecting gravity at the measurement location has a radius of $\sim 1 \text{ km}$ around the gravimeter. Furthermore, we demonstrated that saturated water storage change has a strongly non-linear and state-dependent relationship with gravity.

In order to apply gravity data in hydrological modeling, we have built models according to the classification of water storage changes (fast and slow). The fast storage change has been modeled by a lumped water balance model, the parameters of which were constrained by gravity variation data. The output of the lumped water balance model was then used as the input forcing of a semi-distributed hydraulic groundwater model for the slow storage change. The coupled modeling system successfully reproduced both gravity and discharge dynamics. Our hydrological models explained 80% of the variance of observed gravity residuals.

From a hydrological perspective, terrestrial gravity measurements of the kind used in our study offer an intriguing new look at catchment-scale hydrological processes. Terrestrial gravity observations are interesting to explore in catchment-scale hydrological modeling because of their relation with changes in terrestrial water storage.

6.1.2 Satellite geodesy

To date, neither traditional observation techniques nor land surface models have the capability to quantify the terrestrial water storage (TWS). Observed hydrological data are too sparse and spatial heterogeneity is too strong to provide any reasonable estimate of TWS. Although land surface models may well estimate basin-scale river discharge, the spatio-temporal variability of TWS components cannot be verified. As the only remote sensing system capable of measuring water storage changes at all levels on and below the land surface, GRACE provides an unprecedented opportunity to improve quantification, understanding, and simulation of TWS variability (*Zaitchik et al., 2008*).

In Chapter 5, a comprehensive analysis combining VIC, GRACE and in-situ data has been presented. The spatio-temporally variable relationships between the three products (VIC, GRACE and in-situ data) were examined to find their correlations, and to explain the similarities and differences observed. The three different solutions (CSR, GFZ and JPL) of the GRACE twin satellite mission yielded significantly different results for the same basin. As a result, users should be careful in applying GRACE data. GRACE gravity fields should be

corrected for different errors by using additional data and models. In addition, some kind of smoothing of the data is essential to obtain a meaningful dataset. A spatial smoothing operation on different GRACE estimates brings their results closer together. However, smoothing also raises the question: what essential signal is remaining in a dataset after such a filtering operation?

We found good agreement between the dynamics of basin average VIC simulations and GRACE estimates. While compared separately, the correlations were different for the Upper and Lower Colorado basin, which could be explained. For example, soil moisture and snow are dominant in the Upper Colorado and groundwater is dominant in the Lower Colorado. For the case of snow, a significant correlation was found between GRACE and observed data. VIC simulated storage variations were smoothed in the same way as GRACE and a spatially distributed comparison showed good results. However, to improve our analysis we would need to take into account hydrological information from the surroundings of the basin.

6.2 General discussion

6.2.1 Terrestrial gravity

In Chapter 2, time series analysis has been explored to explain local gravity variation as observed by a superconducting gravimeter. This approach yielded encouraging results, confirming why the hydrological effects on such gravity variations are typically accounted for by finding and applying empirical relations of different (available) hydrometeorological data (precipitation, soil moisture, groundwater) with gravity residuals. Time series analysis is mostly done in both the time and the frequency domain. In our case, we have done this analysis only in the time domain, mainly for the following reason. Measured gravity (or its temporal variation) contains effects of many periodic components of different frequencies and magnitudes. Gravity residuals are obtained by filtering the raw signal for known effects, a number of which are periodic in nature. As a result, frequency domain analyses are already performed in the process of obtaining the gravity residuals.

The availability of digital geographic data, particularly digital elevation models, makes distributed hydrological modeling possible. At the same time, surface heterogeneity and the lack of subsurface data makes the modeling difficult. The Soil Moisture Routing (SMR) model was developed specifically for topographically steep areas, hydrologically characterized by relatively thin, permeable soil layers over a much less permeable fragipan, bedrock, or other restricting layer. The model is most effective where slopes are steep enough to be the main cause of lateral flow. SMR application is limited to regions fitting the description discussed above and should not be viewed as a generally applicable hydrological model. In Chapter 3, a distributed hydrological modeling technique was explored to explain local gravity variations. Distributed water balance modeling explained both short and long-term behavior of the gravity

signal. The hydrological model also confirms the findings from our time series analysis (Chapter 2). The periods (winter months: November - February) of high positive correlation between groundwater and gravity changes (Chapter 2) were found to coincide with the periods where modeled gravity variations do not behave as observed gravity residuals (Chapter 3). On the one hand, the SMR model suffered from the lack of distributed data. On the other hand, it clearly demonstrated what are the important parameters to be considered to model hydrological gravity variations.

Mass changes cause changes in gravity in two ways. First, by the gravitational attraction of the changed mass and second, by the vertical crustal motion (hence, physical displacement or change of location) caused by the changed mass. We did not consider any vertical crustal motion in our analysis mainly because the gravimeter was located on the bedrock, which makes the vertical crustal motion negligible.

In Chapter 4, we employed terrestrial gravity observations from a single location to constrain hydrological models in a small catchment. To do that, our hydrological model had to match the gravity dynamics. For example, a simple lumped water balance model was enough to model the short-term hydrological conditions, constrained by fast and short-term gravity variations. This provided us with robust and effective input conditions for the semi-distributed hillslope-storage Boussinesq (hsB) model to successfully reproduce the discharge magnitude and dynamics. Despite the fact that the parameters used in the lumped water balance model are averaged over the entire catchment, our models gave encouraging results for both hydrology and gravity. Considering the observed gravity change as an additional integrator of catchment-scale hydrological response, and therefore using it to constrain hydrologic models for that catchment, provides a new way of validating water balance estimates.

Geographical position relative to the gravimeter plays an important role in the relationship between storage and gravity variation. The topography-based analysis, using an available DEM and possible storage variations distributed in the catchment, shows the extent of the hydrological domain affecting point-scale gravity. Despite the encouraging results we obtained in hydrological modeling, Chapter 4 also showed the limitations of the local geophysical conditions on modeling of temporal gravity variation caused by hydrological redistribution, where storage changes occur both above and below a gravimeter. However, by providing the likely range of variation in gravity caused by local hydrological changes, we were able to produce a gravity time series free from local hydrological effects.

Hinderer et al. (2006) investigated seasonal changes of the earth's gravity field from GRACE, and made a comparison with surface gravity measurements in Europe from the GGP network and hydrological models for continental soil moisture and snow. Following their findings and discussions, terrestrial gravity variations observed at the point-scale have to be free from local effects, in order to be applicable in larger-scale hydrological investigations. In Chapter 4, we provided calculations of gravity variations caused by local hydrological changes that explain 80% of the observed gravity variations.

Considering the influence of complex geophysical conditions and limited knowledge of sub-surface variability in detecting local hydrological effects on gravity, satellite geodesy has the potential of simplifying the geophysical conditions to some extent. For example, the issues related to topographical locations (above or below the gravimeter) raised above are valid for ground-based gravity measurements. For satellite-based measurements of the gravity potential, all hydrological processes take place below the instrument (satellite).

6.2.2 Satellite geodesy

The success of macroscale hydrological models depends on how accurately spatially variable model parameters and input forcings represent the true basin conditions. By analyzing basin scale hydrology and storage change related estimates from GRACE (Chapter 5), we showed what we essentially need or what is currently missing to apply GRACE in hydrological studies. From the same raw data of the GRACE twin satellite mission, three products are generated, which are quite different. These differences between the various GRACE products for the same basin also need to be addressed. Although it is understandable that the three science data centers perform their own calculations based on the application of different data reduction models, for the users of GRACE in general and for the hydrological community in particular the issue of these differences will remain a problem to be solved before GRACE data can be routinely applied in their studies.

Because of the spatial scale of the basin we studied, we may have to decide that GRACE data is not yet suitable at such a relatively small scale. Nevertheless, the agreement between GRACE, VIC and in-situ data in the Colorado River Basin provided some confirmation that our VIC model was appropriate for modeling the hydrology and that the meteorological forcing we employed could be considered adequate. However, the limited agreement regarding the amplitude may raise questions about the calibrated model parameters, as well as applicability of GRACE in the CRB, given its size and water storage variability. Although the model performance in terms of simulated discharge was found to be good, the storage distribution and dynamics do not have to reflect the true conditions.

6.3 Perspectives

Application of gravity observations in hydrological studies is still in its infancy. Hence, a lot is still to be done before gravity can be routinely used as a remote sensor. A logical first step would be to improve our knowledge and understanding of temporal and spatial variations of and relations between terrestrial water storage components. This can form the basis for a reasonable description of mass redistribution processes in the hydrological cycle for current conditions and consequently also for reliable estimates of the future developments by scenario simulations. The above mentioned recommendation

is valid at both catchment and basin scale.

Basin scale hydrological studies are needed to investigate the possibilities for GRACE data assimilation in hydrological modeling. Soil moisture is variable in space and time and many moisture dependent processes are nonlinear. This leads to scale effects that need to be understood if we are to make accurate predictions of the behavior of hydrologic systems, where it is generally necessary to aggregate in space and/or time. Similarly, many other spatial and temporal fields (e.g. soil, vegetation, topography, meteorology) that influence soil moisture and other hydrologic responses are variable. The consequence of this is that scale effects are complex, making hydrologic simulation and prediction very challenging. At present, an investigation addressing the scale issues involved in application of gravity data in hydrological modeling, is missing. Such an investigation would improve application of geophysical data in hydrologic studies.

GRACE provides a temporal and spatial average estimate of geoid change, which can subsequently be translated to (a temporal and spatial average estimate of) continental water storage change. What GRACE provides is a new kind of data for hydrology. As a result, we need to look for new ways of modeling the terrestrial water storage to exploit GRACE data in hydrological modeling. The main question reduces to what a temporal and spatial average estimate of continental water storage change means in terms of representing hydrological processes in a catchment, and how different water storage components play their roles in affecting total water storage change.

Bibliography

- Allen, R. G. (2000), *REF-ET Reference Evapotranspiration Calculator*, University of Idaho, Kimberly, Idaho, available online <http://www.kimberly.uidaho.edu/ref-et/>.
- Alsdorf, D. E., and D. P. Lettenmaier (2003), Tracking fresh water from space, *Science*, *301*(5639), 1491–1494.
- Bales, R. C., N. P. Molotch, T. H. Painter, M. D. Dettinger, R. Rice, and J. Dozier (2006), Mountain hydrology of the western United States, *Water Resour. Res.*, *42*, W08432, doi:10.1029/2005WR004387.
- Bastiaanssen, W. G. M., H. Pelgrum, P. Droogers, H. A. R. de Bruin, and M. Menenti (1997), Area-average estimates of evaporation, wetness indicators and top soil moisture during two golden days in EFEDA, *Agr. Forest Meteorol.*, *87*(2-3), 119–137.
- Boll, J., E. S. Brooks, C. R. Campbell, C. O. Stockle, S. K. Young, J. E. Hammel, and P. A. McDaniel (1998), Progress toward development of a GIS based water quality management tool for small rural watersheds: Modification and application of a distributed model, paper presented at the 1998 ASAE Annual International Meeting in Orlando, Florida, July 12-16, Paper 982230, ASAE, 2950 Niles Road, St. Joseph, MI.
- Boronina, A., and G. Ramillien (2008), Application of AVHRR imagery and GRACE measurements for calculation of actual evapotranspiration over the Quaternary aquifer (Lake Chad Basin) and validation of groundwater models, *J. Hydrol.*, *348*(1-2), 98–109, doi:10.1016/j.jhydrol.2007.09.061.
- Bower, D. R., and N. Courtier (1998), Precipitation effects on gravity measurements at the Canadian absolute gravity site, *Phys. Earth Planet. In.*, *106*(3-4), 353–369.
- Box, G. E. P., and G. M. Jenkins (1976), *Time Series Analysis: Forecasting and Control*, 575 pp., Holden-Day, San Francisco, USA.

- Campbell, G. S. (1974), A simple method for determining unsaturated conductivity from moisture retention data, *Soil Sci.*, 117(6), 311–314.
- Chambers, D. P. (2006), Evaluation of new GRACE time-variable gravity data over the ocean, *Geophys. Res. Lett.*, 33, L17603, doi:10.1029/2006GL027296.
- Chao, B. F. (1994), The geoid and earth rotation, in *Geoid and Its Geophysical Interpretations*, edited by P. Vanicek and N. T. Christou, pp. 285–298, CRC Press, Boca Raton, USA.
- Christensen, N. S., A. W. Wood, N. Voisin, D. P. Lettenmaier, and R. N. Palmer (2004), The effects of climate change on the hydrology and water resources of the Colorado River Basin, *Climatic Change*, 62(1-3), 337–363, doi:10.1023/B:CLIM.0000013684.13621.1f.
- Clapp, R., and G. Hornberger (1978), Empirical equations for some soil hydraulic properties, *Water Resour. Res.*, 14(4), 601604.
- Crossley, D., et al. (1999), Network of superconducting gravimeters benefits several disciplines, *EOS Trans. AGU*, 80, 121–126.
- Crossley, D. J., and S. Xu (1998), Analysis of superconducting gravimeter data from Table Mountain, Colorado, *Geophys. J. Int.*, 135(3), 835–844.
- Farrell, W. E. (1972), Deformation of the earth by surface loads, *Rev. Geophys.*, 10(3), 761–797.
- Frankenberger, J. R., E. S. Brooks, M. T. Walter, M. F. Walter, and T. S. Steenhuis (1999), A GIS-based variable source area hydrology model, *Hydrol. Proceses.*, 13, 805–822.
- Goodkind, J. M. (1999), The superconducting gravimeter, *Rev. Sci. Instrum.*, 70(11), 4131–4152.
- Güntner, A. (2008), Improvement of global hydrological models using GRACE data, *Surv. Geophys.*, doi:10.1007/s10712-008-9038-y.
- Harnisch, M., and G. Harnisch (2002), Seasonal variations of hydrological influences on gravity measurements at Wettzell, *Bull. Inform. Marées Terr.*, 137, 10,849–10,861.
- Hasan, S., P. A. Troch, J. Boll, and C. Kroner (2006), Modeling the Hydrological Effect on Local Gravity at Moxa, Germany, *J. Hydrometeorol.*, 7(3), 346–354, doi:10.1175/JHM488.1.
- Hasan, S., P. A. Troch, P. W. Bogaart, and C. Kroner (2008), Evaluating catchment-scale hydrological modeling by means of terrestrial gravity observations, *Water Resour. Res.*, 44, W08416, doi:10.1029/2007WR006321.
- Hinderer, J., O. B. Andersen, F. Lemoine, D. Crossley, and J. P. Boy (2006), Seasonal changes in the European gravity field from GRACE: A comparison with superconducting gravimeters and hydrology model predictions, *J. Geodyn.*, 41(1-3), 59–68, doi:10.1016/j.jog.2005.08.037.
- Jackson, T. J., D. M. Le Vine, A. Y. Hsu, A. Oldak, P. J. Starks, C. T. Swift, J. D. Isham, and M. Haken (1999), Soil moisture mapping at regional scales using microwave radiometry: The Southern Great Plains Hydrology Experiment, *IEEE T. Geosci. Remote Sensing*, 37(5), 2136–2151.

- Jensen, M. E. (1973), *Consumptive Use of Water and Irrigation Water Requirements*, 215 pp., ASCE, New York, USA.
- Kimball, H. H. (1924), Records of total solar radiation intensity and their relation to daylight intensity, *Mon. Weather Rev.*, 52(10), 473–479.
- Krajewski, W. F., et al. (2006), A remote sensing observatory for hydrologic sciences: A genesis for scaling to continental hydrology, *Water Resour. Res.*, 42, W07301, doi:10.1029/2005WR004435.
- Kroner, C. (2001), Hydrological effects on gravity at the Geodynamic Observatory Moxa, *J. Geod. Soc. Japan*, 47(1), 353–358.
- Kroner, C., and G. Jentzsch (1999), Comparison of different barometric pressure reductions for gravity data and resulting consequences, *Phys. Earth Planet. In.*, 115(3-4), 205–218.
- Kroner, C., T. Jahr, and G. Jentzsch (2004), Results from 44 months of observations with a superconducting gravimeter at Moxa/Germany, *J. Geodyn.*, 38(3-5), 263–280.
- Lankreijer, H., A. Lundberg, A. Grelle, A. Lindroth, and J. Seibert (1999), Evaporation and storage of intercepted rain analysed by comparing two models applied to a boreal forest, *Agric. Forest Meteorol.*, 98-99, 595–604.
- Liang, X., D. P. Lettenmaier, E. F. Wood, and S. J. Burges (1994), A simple hydrologically based model of land surface water and energy fluxes for general circulation models, *J. Geophys. Res.*, 99(D7), 14,415–14,428.
- List, R. J. (1968), *Smithsonian Meteorological Tables*, 114, sixth ed., 527 pp., Smithsonian Institution Press, Washington, USA.
- Mäkinen, J., and S. Tattari (1988), Soil moisture and groundwater: Two sources of gravity variations, *Bull. Inform. Marées Terr.*, 62, 103–110.
- Mancini, M., R. Hoeben, and P. A. Troch (1999), Multifrequency radar observations of bare surface soil moisture content: A laboratory experiment, *Water Resour. Res.*, 36(6), 1827–1838.
- Maurer, E. P., A. W. Wood, J. C. Adam, D. P. Lettenmaier, and B. Nijssen (2002), A long-term hydrologically based dataset of land surface fluxes and states for the conterminous United States, *J. Climate*, 15(22), 3237–3251.
- Nagy, D. (1966), The gravitational attraction of a right rectangular prism, *Geophysics*, 31, 362–371.
- Nash, J. E., and J. V. Sutcliffe (1970), River flow forecasting through conceptual models, part I – A discussion of principles, *J. Hydrol.*, 10(3), 282–290.
- Ngo-Duc, T., K. Laval, G. Ramillien, J. Polcher, and A. Cazenave (2007), Validation of the land water storage simulated by Organising Carbon and Hydrology in Dynamic Ecosystems (ORCHIDEE) with Gravity Recovery and Climate Experiment (GRACE) data, *Water Resour. Res.*, 43, W04427, doi:10.1029/2006WR004941.
- Niu, G., and Z. Yang (2006), Assessing a land surface model's improvements with GRACE estimates, *Geophys. Res. Lett.*, 33, L07401, doi:10.1029/2005GL025555.

- Niu, G. Y., K. W. Seo, Z. L. Yang, C. Wilson, H. Su, J. Chen, and M. Rodell (2007), Retrieving snow mass from GRACE terrestrial water storage change with a land surface model, *Geophys. Res. Lett.*, *34*, L15704, doi: 10.1029/2007GL030413.
- Njoku, E. G., and L. Li (1999), Retrieval of land surface parameters using passive microwave measurements at 6–18 GHz, *IEEE T. Geosci. Remote Sensing*, *37*(1), 79–93.
- NRC (1997), Satellite gravity and the geosphere, *Tech. rep.*, National Research Council, Washington D. C. , USA.
- Peixoto, J. P., and A. H. Oort (1992), *Physics of Climate*, 520 pp., Springer, New York, USA.
- Peter, G., P. G. Klopping, and K. A. Berstis (1995), Observing and modeling gravity changes caused by soil moisture and groundwater table variations with superconducting gravimeters in Richmond, Florida, USA., *Cahier du Centre Européen de Géodynamique et de Séismologie*, *11*, 147–159.
- Pool, D. R. (2005), Variations in climate and ephemeral channel recharge in southeastern Arizona, United States, *Water Resour. Res.*, *41*, W11403, doi: 10.1029/2004WR003255.
- Pool, D. R., and J. H. Eychaner (1995), Measurements of aquifer-storage change and specific yield using gravity surveys, *Ground Water*, *33*(3), 425432, doi: 10.1111/j.1745-6584.1995.tb00299.x.
- Prairie, J., and R. Callejo (2005), Natural flow and salt computation methods, *Tech. rep.*, U.S. Department of the Interior, Bureau of Reclamation, Salt Lake City, Utah.
- Priestley, M. B. (1981), *Spectral Analysis and Time Series*, first ed., 890 pp., Academic Press, London, UK.
- Ramillien, G., F. Frappart, A. Cazenave, and A. Güntner (2005), Time variations of land water storage from an inversion of 2 years of GRACE geoids, *Earth Planet. Sc. Lett.*, *235*(1-2), 283–301, doi:10.1016/j.epsl.2005.04.005.
- Ramillien, G., F. Frappart, A. Güntner, T. Ngo-Duc, A. Cazenave, and K. Laval (2006), Time variations of the regional evapotranspiration rate from Gravity Recovery and Climate Experiment (GRACE) satellite gravimetry, *Water Resour. Res.*, *42*, W10403, doi:10.1029/2005WR004331.
- Rodell, M., and J. S. Famiglietti (1999), Detectability of variations in continental water storage from satellite observations of the time dependent gravity field, *Water Resour. Res.*, *35*(9), 2705–2724.
- Rodell, M., and J. S. Famiglietti (2001), An analysis of terrestrial water storage variations in Illinois with implications for the Gravity Recovery And Climate Experiment (GRACE), *Water Resour. Res.*, *37*(5), 1327–1340.
- Rodell, M., and J. S. Famiglietti (2002), The potential for satellite-based monitoring of groundwater storage changes using GRACE: The High Plains aquifer, Central US, *J. Hydrol.*, *263*(1-4), 245–256, doi:10.1016/S0022-1694(02)00060-4.

- Rodell, M., J. S. Famiglietti, J. Chen, S. I. Seneviratne, P. Viterbo, S. Holl, and C. R. Wilson (2004), Basin scale estimates of evapotranspiration using GRACE and other observations, *Geophys. Res. Lett.*, *31*, L20504, doi:10.1029/2004GL020873.
- Schutz, B. (2003), *Gravity from the Ground Up*, first ed., 462 pp., Cambridge University Press, Cambridge, UK.
- Su, Z. (2002), The Surface Energy Balance System (SEBS) for estimation of turbulent heat fluxes, *Hydrol. Earth Syst. Sc.*, *6*(1), 85–99.
- Su, Z., P. A. Troch, and F. P. de Troch (1997), Remote sensing of bare surface soil moisture using EMAC/ESAR data, *Int. J. Remote Sens.*, *18*(10), 2105–2124.
- Swenson, S., and J. Wahr (2002), Methods for inferring regional surface-mass anomalies from Gravity Recovery and Climate Experiment (GRACE) measurements of time-variable gravity, *J. Geophys. Res.*, *107*(B9), 2193, doi:10.1029/2001JB000576.
- Swenson, S., J. Wahr, and P. C. D. Milly (2003), Estimated accuracies of regional water storage variations inferred from the Gravity Recovery and Climate Experiment (GRACE), *Water Resour. Res.*, *39*(8), 1223, doi:10.1029/2002WR001808.
- Swenson, S., P. J.-F. Yeh, J. Wahr, and J. Famiglietti (2006), A comparison of terrestrial water storage variations from GRACE with in situ measurements from Illinois, *Geophys. Res. Lett.*, *33*, L16401, doi:10.1029/2006GL026962.
- Swenson, S., D. Chambers, and J. Wahr (2008), Estimating geocenter variations from a combination of GRACE and ocean model output, *J. Geophys. Res.*, *113*, B08410, doi:10.1029/2007JB005338.
- Swenson, S. C., and P. C. D. Milly (2006), Climate model biases in seasonality of continental water storage revealed by satellite gravimetry, *Water Resour. Res.*, *42*, W03201, doi:10.1029/2005WR004628.
- Syed, T. H., J. S. Famiglietti, J. Chen, M. Rodell, S. I. Seneviratne, P. Viterbo, and C. R. Wilson (2005), Total basin discharge for the Amazon and Mississippi River basins from GRACE and a land-atmosphere water balance, *Geophys. Res. Lett.*, *32*, L24404, doi:10.1029/2005GL024851.
- Tapley, B. D., S. Bettadpur, J. C. Ries, P. F. Thompson, and M. M. Watkins (2004a), GRACE measurements of mass variability in the earth system, *Science*, *305*(5683), 503–505, doi:10.1126/science. 1099192.
- Tapley, B. D., S. Bettadpur, M. Watkins, and C. Reigber (2004b), The gravity recovery and climate experiment: Mission overview and early results, *Geophys. Res. Lett.*, *31*, L09607, doi:10.1029/2004GL019920.
- Teuling, A. J., and P. A. Troch (2005), Improved understanding of soil moisture variability dynamics, *Geophys. Res. Lett.*, *32*, L05404, doi:10.1029/2004GL021935.
- Teupser, C. (1975), The seismological station of Moxa, *Veröff. Zentralinst. Physik d. Erde*, *31*, 577–584.

- Thornthwaite, C. W., and J. R. Mather (1955), *The water balance, Publications in climatology / Laboratory of Climatology*, vol. 8(1), 86 pp., Centerton: Drexel Institute of Technology, New Jersey, USA.
- Torge, W. (1989), *Gravimetry*, 465 pp., de Gruyter, Berlin, Germany.
- Torge, W. (2001), *Geodesy: An Introduction*, third ed., 416 pp., Walter de Gruyter, Berlin, Germany.
- Troch, P., M. Durcik, S. Seneviratne, M. Hirschi, A. Teuling, R. Hurkmans, and S. Hasan (2007), New data sets to estimate terrestrial water storage change, *EOS Trans. AGU*, 88(45), 469–470.
- Troch, P. A., C. Paniconi, and D. McLaughlin (2003a), Catchment-scale hydrological modeling and data assimilation, *Adv. Water Resour.*, 26(2), 131–135.
- Troch, P. A., C. Paniconi, and E. E. van Loon (2003b), Hillslope-storage Boussinesq model for subsurface flow and variable source areas along complex hillslopes: 1. Formulation and characteristic response, *Water Resour. Res.*, 39(11), 1316, doi:10.1029/2002WR001728.
- Turcotte, D. L., and G. Schubert (2002), *Geodynamics*, second ed., 456 pp., Cambridge University Press, Cambridge, UK.
- Van Camp, M., M. Vanclooster, O. Crommen, T. Petermans, K. Verbeeck, B. Meurers, T. van Dam, and A. Dassargues (2006), Hydrogeological investigations at the Membach station, Belgium, and application to correct long periodic gravity variations, *J. Geophys. Res.*, 111, B10403, doi:10.1029/2006JB004405.
- Verhoest, N. E. C., P. A. Troch, C. Paniconi, and F. P. de Troch (1998), Mapping basin scale variable source areas from multitemporal remotely sensed observations of soil moisture behavior, *Water Resour. Res.*, 34(12), 3235–3244.
- Wahr, J., M. Molenaar, and F. Bryan (1998), Time variability of the earth's gravity field: Hydrological and oceanic effects and their possible detection using GRACE, *J. Geophys. Res.*, 103(B12), 30,205–30,230.
- Wahr, J., S. Swenson, V. Zlotnicki, and I. Velicogna (2004), Time-variable gravity from GRACE: First results, *Geophys. Res. Lett.*, 31, L11501, doi:10.1029/2004GL019779.
- Werth, S., A. Güntner, S. Petrovic, and R. Schmidt (2009), Integration of GRACE mass variations into a global hydrological model, *Earth Planet. Sc. Lett.*, 277(1-2), 283–301, doi:10.1016/j.epsl.2008.10.021.
- Zaitchik, B. F., M. Rodell, and R. H. Reichle (2008), Assimilation of GRACE terrestrial water storage data into a land surface model: Results for the Mississippi River Basin, *J. Hydrometeorol.*, 9(3), 535–548, doi:10.1175/2007JHM951.1.

Hydrological research is currently going through a revolution, in which a multitude of new data sources and knowledge from other branches of geoscience are being applied, explored, and tested. One example of these new kinds of data is highly accurate temporal gravity variations from both ground-based and spaceborne observations. Ground-based observations are done by superconducting gravimeters that provide extremely accurate data on temporal gravity variations, from which hydrological signals can be captured. The twin satellites from the Gravity Recovery and Climate Experiment (GRACE) are making detailed measurements of the earth's gravity field with unprecedented accuracy, from which mass variations on and below the earth's surface due to geophysical processes can be deduced.

Terrestrial water storage is a key factor in the water cycle and of direct influence to all hydrological and related processes. Therefore it plays a major role in climate modeling and water management issues. This thesis aims at investigating the possibility to detect variations in terrestrial water storage from measurements of the time dependent gravity field, based on terrestrial (superconducting gravimeters) and satellite (GRACE) observations of the gravity field. The hypothesis is that temporally variable gravity measurements, both terrestrial and satellite based, contain valuable information about water storage in surface and subsurface reservoirs (e.g. snow, soil moisture, groundwater).

Chapter 2 describes time series analysis and modeling of terrestrial gravity. Gravity residuals were analyzed with precipitation, groundwater and temperature data from the Geodynamic Observatory, Moxa, Germany. It is shown that precipitation has a direct effect on gravity, which can be modeled by a simple impulse response function. Analysis of groundwater and gravity demonstrates different kinds of dynamics present in the catchment around the gravimeter.

Chapter 3 presents an application of a distributed hydrological model to model terrestrial gravity variation. Driven by observed atmospheric forcings, the model computes the variation of different water storage components. These water storage variations are then converted to predicted gravity variation at the location of

the superconducting gravimeter and compared to observed gravity residuals. Distributed water balance modeling explains both short and long-term behavior of the gravity signal. The hydrological model also confirms the findings from the time series analysis and modeling (Chapter 2).

Chapter 4 demonstrates an application of observed gravity residuals in hydrological modeling. Simple water balance models are used to simulate catchment water storage dynamics, where the dynamics is classified into fast and slow changes. The fast storage change has been modeled by a lumped water balance model, the parameters of which were constrained by gravity variation data. The output of the lumped water balance model is then used as the input forcing of a semi-distributed hydraulic groundwater model for the slow storage change. The coupled modeling system successfully reproduces both gravity and discharge dynamics. By means of a sensitivity analysis, it is also shown what parts of the gravity variation can be estimated from hydrological models.

Chapter 5 describes a comprehensive analysis combining a basin-scale hydrological model, GRACE and in-situ data. The spatio-temporally variable relationships between these three products are examined to find their correlations, and to explain the similarities and differences observed. Although a good agreement between the basin average dynamics of the hydrological model and GRACE data exists, care has to be taken in applying GRACE data at the small basin scale with a single model. Nevertheless, this analysis shows the potential of GRACE and provides new questions regarding large scale hydrological modeling.

Application of gravity observations in hydrological studies is still in its infancy. Hence, a lot is still to be done before gravity can be routinely used as a remote sensor. A logical first step is to improve our knowledge and understanding of temporal and spatial variations of and relations between terrestrial water storage components. This can form the basis for a reasonable description of mass redistribution processes in the hydrological cycle for current conditions and consequently also for reliable estimates of the future developments by scenario simulations. Both ground-based and spaceborne observations of temporal gravity variations, such as used in this thesis, offer an intriguing new look at catchment and basin-scale hydrological processes.

Samenvatting

Er is momenteel een revolutie gaande in hydrologisch onderzoek, waarbij een massa nieuwe gegevens en kennis uit andere aardwetenschappelijke disciplines wordt toegepast, onderzocht en getest. Een voorbeeld van deze nieuwe gegevens is de zeer nauwkeurige temporele zwaartekrachtvariatie, waargenomen op basis van zowel veld- als satellietwaarnemingen. Vanuit de veldwaarnemingen die met behulp van supergeleidende gravimeters worden gedaan, en die bijzonder nauwkeurige temporele zwaartekrachtvariatiegegevens weergeven, kan een hydrologisch signaal worden afgeleid. De tweelingsatellieten van de internationale zwaartekrachtmissie 'Gravity Recovery and Climate Experiment' (GRACE) doen gedetailleerde metingen van het zwaartekrachtveld van de aarde met een tot dusver ongekende nauwkeurigheid, op basis waarvan massavariaties op en onder het aardoppervlak ten gevolge van geofysische processen kunnen worden vastgesteld.

Waterberging in en op de aarde (terrestrische wateropslag) is een belangrijke component van de waterkringloop en rechtstreeks van invloed op alle hydrologische en aanverwante processen. Daarom speelt deze een belangrijke rol in klimaatmoderling en waterbeheerskwesties. Dit proefschrift heeft als doel om de verschillen vast te stellen tussen de variaties in terrestrische wateropslag en metingen van het tijdsafhankelijke zwaartekrachtveld. Dit is gebaseerd op terrestrische (supergeleidende gravimeters) en satelliet (GRACE) waarnemingen van het zwaartekrachtveld. De hypothese is dat temporeel veranderlijke zwaartekrachtmetingen, zowel de terrestrische als de satellietwaarnemingen, waardevolle informatie bevatten over wateropslag aan het aardoppervlak en in de bodem (b.v. sneeuw, bodemvocht, grondwater).

Hoofdstuk 2 beschrijft tijdreeksanalyse en modelering van terrestrische zwaartekracht. Variaties in de gemeten zwaartekracht zijn met neerslag-, grondwater- en temperatuurgegevens van het 'Geodynamic Observatory' in Moxa, Duitsland, vergeleken. Hiermee is aangetoond dat neerslag een rechtstreeks effect op de zwaartekracht heeft, die door een eenvoudige impulsresponsfunctie kan worden gemodelleerd. Analyse van grondwater en zwaartekracht demonstreert de verschillen

in dynamiek aanwezig in het afwateringsreservoir rond de gravimeter.

Hoofdstuk 3 presenteert de toepassing van een ruimtelijk verdeeld hydrologisch model om aardse zwaartekrachtvariaties te modelleren. Op basis van atmosferische waarnemingen berekent het model de variatie van verschillende wateropslagcomponenten. De dynamiek in wateropslag is vervolgens naar voorspelde zwaartekrachtvariatie op de locatie van de supergeleidende gravimeter omgezet en vergeleken met waargenomen residuele zwaartekrachtvariaties. Modelering van de waterbalans verklaart zowel korte als langetermijngedragingen van het zwaartekrachtsignaal. Het hydrologisch model bevestigt ook de bevindingen van de tijdreeksanalyse en modelering (Hoofdstuk 2).

Hoofdstuk 4 demonstreert een toepassing van de waargenomen residuele zwaartekracht in een hydrologisch model. Eenvoudige waterbalansmodellen zijn gebruikt om de dynamiek in wateropslag op stroomgebiedsniveau te simuleren, waarbij deze is onderverdeeld in snelle en langzame veranderingen. De snelle opslagverandering is door middel van een ruimtelijk geaggregeerd waterbalansmodel gemodelleerd, waarvan de parameters door zwaartekrachtvariatiegegevens zijn bepaald. De uitkomsten van het waterbalansmodel zijn vervolgens gebruikt als de invoergegevens van een semi-verdeeld hydraulisch grondwatermodel waarmee de langzame opslagverandering bepaald is. Het gekoppelde modelsysteem reproduceert succesvol zowel de zwaartekracht- als de afvoerdynamiek. Door middel van een gevoeligheidsanalyse is ook getoond welke delen van de zwaartekrachtvariatie met behulp van hydrologische modellen kunnen worden geschat.

Hoofdstuk 5 beschrijft een veelomvattende analyse waarbij een hydrologisch model op stroomgebiedsschaal, GRACE- en in-situ gegevens worden gecombineerd. De als functie van tijd en plaats veranderlijke verhoudingen tussen deze drie elementen zijn onderzocht om correlaties te vinden en de waargenomen overeenkomsten en verschillen te verklaren. Hoewel er een goede overeenkomst tussen de stroomgebiedsdynamiek van het hydrologisch model en GRACE-gegevens is gevonden, dient men voorzichtig te zijn met het toepassen van GRACE-gegevens in kleinschalige stroomgebieden ten behoeve van modellering met een enkel model. Niettemin toont deze analyse het potentieel van GRACE aan, hetgeen leidt tot nieuwe vragen aangaande grootschalige hydrologische modelering.

De toepassing van zwaartekrachtwaarnemingen in hydrologisch onderzoek is nog in een beginstadium. Er is daarom nog veel te doen voordat zwaartekracht routinematig kan worden gebruikt als 'remote sensor' (instrument voor teledetectie). Een logische eerste stap is het verbeteren van onze kennis omtrent tijd- en plaatsgebonden variaties van en relaties tussen terrestrische waterbalanscomponenten. Dit kan de basis vormen voor een goed onderbouwde beschrijving van massaherverdelingsprocessen in de hydrologische cyclus onder de huidige omstandigheden en daarna ook voor betrouwbare schattingen van de toekomstige ontwikkelingen door middel van scenariosimulaties. Zowel de terrestrische- als de satellietwaarnemingen van temporele zwaartekrachtvariaties, zoals gebruikt in dit proefschrift, bieden een intrigerend nieuw perspectief op hydrologische processen op stroomgebiedsschaal.

PhD training program

Fulfilled all requirements of the educational PhD program of the Netherlands Research School for the Socio-Economic and Natural Sciences of the Environment (SENSE), with the following activities:

SENSE PhD courses:

- Environmental Research in Context
- Research Context Activity: "Highlight article in Annual Report 2003 of Wageningen Institute for Environment and Climate Research (WIMEK), Netherlands"
- Uncertainty Modelling and Analysis

Other Phd courses:

- Climate and the Hydrological Cycle
- Scientific Writing

Research and Management Skills:

- Introduction to satellite geodesy (GRACE) in the context of hydrological studies, University California, Irvine (UCI), USA
- Application of GRACE in Hydrology, Institute of Water Modelling (IWM), Bangladesh

Oral Presentations:

- AGU Fall meeting, December 2003, San Francisco, USA
- 15th International Symposium on Earth Tides, August 2004, Ottawa, Canada
- CAHMDA-II International Workshop, October 2004, Princeton, USA
- SENSE Summer Symposium, June 2005, Ede, The Netherlands

Curriculum Vitae

Shaakeel Hasan, 22 September 1968, Kushtia, Bangladesh

- 1984
Secondary School Certificate (SSC), Kushtia Zilla School, Bangladesh.
- 1986
Higher Secondary Certificate (HSC), Kushtia Government College, Bangladesh.
- 1992
BSc in Civil Engineering, Bangladesh Institute of Technology (BIT), Rajshahi, Bangladesh.
- 1993 – 1996
Field Engineer, Bangladesh Engineering and Technological Services (BETS) Ltd., Tangail, Bangladesh.
- 1996 – 1997
GIS Expert, Bangladesh Engineering and Technological Services (BETS) Ltd., Dhaka, Bangladesh.
- 1998 – 1999
Civil Engineer & GIS Expert, Engineers International, Gaborone, Botswana.
- 2001
MSc in Hydroinformatics, International Institute for Infrastructural, Hydraulic and Environmental Engineering (IHE), Delft, Netherlands.
- 2001 – 2002
Temporary Researcher, Hydroinformatics and Knowledge Management (HIKM), UNESCO-IHE, Delft, Netherlands.
- 2003 – 2007
Trainee Research Assistant (AIO), Hydrology and Quantitative Water Management, Wageningen University, Netherlands.
- 2008 – present
Researcher, Institute of Marine and Atmospheric research Utrecht (IMAU), Utrecht University, Netherlands.